Mechanisms of *Trichodesmium* demise within the New Caledonian lagoon during the VAHINE mesocosm experiment

D. Spungin[1], U. Pfreundt[2], H. Berthelot[3], S. Bonnet[3,4], D. AlRoumi[5], F. Natale[5], W.R. Hess[2], K.D. Bidle[5], I. Berman-Frank[1]

[1] {The Mina and Everard Goodman Faculty of Life Sciences, Bar-Ilan University, Ramat-Gan, Israel}
[2] {University of Freiburg, Faculty of Biology, Schänzlestr. 1, D-79104 Freiburg, Germany}
[3] {Aix Marseille Université, CNRS/INSU, Université de Toulon, IRD, Mediterranean Institute of Oceanography (MIO) UM 110, 13288, Marseille, France}
[4] {Institut de Recherche pour le Développement (IRD), AMU/CNRS/INSU, Université de Toulon, Mediterranean Institute of Oceanography (MIO) UM 110, 13288, Marseille-Noumea, France-New Caledonia}
[5] {Department of Marine and Coastal Sciences, Rutgers University, New Brunswick, NJ, USA}

Correspondence to: I. Berman-Frank (ilana.berman-frank@biu.ac.il)

Abstract

The globally important marine diazotrophic cyanobacterium *Trichodesmium* is seasonally abundant in the New Caledonian lagoon (in the Southwestern Pacific ocean) during austral spring/summer. We investigated the cellular processes mediating *Trichodesmium* mortality from large surface accumulations (blooms) of *Trichodesmium* in the lagoon. *Trichodesmium* cells (and associated microbiota) were collected at the time of surface accumulation, enclosed under simulated ambient conditions, and sampled over time to elucidate the stressors and subcellular underpinning of rapid (~ 24 h) biomass demise (> 90 % biomass) and disappearance occurring in these conditions. Metatranscriptomic profiling of *Trichodesmium* biomass 8 h and 22 h after bottle incubation of surface accumulations demonstrated upregulation expression of genes required to increase phosphorus (P) and iron (Fe) availability and transport. In contrast, genes responsible for nutrient storage were downregulated. Total viral abundance, oscillated throughout the experiment and showed no significant relationship with the development or demise of the *Trichodesmium* biomass. Enhanced caspase-specific activity and upregulated expression of a suite of metacaspase genes as the *Trichodesmium* biomass crashed implicated autocatalytic programmed cell death (PCD) as the mechanistic cause. Concurrently, genes associated with buoyancy and gas-vesicle production were strongly downregulated concomitant with increased production and high concentrations of transparent exopolymeric particles (TEP). The rapid, PCD-mediated, decline of the *Trichodesmium* biomass, as we observed from our incubations, parallels mortality rates reported from *Trichodesmium* blooms *in situ*. Our results suggest that, whatever the ultimate factor, PCD-mediated death in *Trichodesmium* can rapidly terminate blooms, facilitate aggregation, and expedite vertical flux to depth.

1 Introduction

The filamentous N_2-fixing (diazotrophic) cyanobacteria *Trichodesmium* spp. are important contributors to marine N_2 fixation as they form massive blooms (surface accumulations with high biomass density) throughout the oligotrophic marine sub-tropical and tropical oceans (Capone et al., 2004; Capone and Carpenter, 1982; Capone et al., 1997). These surface blooms with densities of 3000 to > 10,000 trichomes L^{-1} and chlorophyll *a* (Chl *a*) concentrations ranging from 1-5 mg L^{-1} develop swiftly and are characterized by high rates of CO_2 and N_2 fixation (Capone et al., 1998; Luo et al., 2012; Rodier and Le Borgne, 2008; Rodier and Le Borgne, 2010). *Trichodesmium* blooms also occur frequently during austral summer between November and March over large areas of the New Caledonian lagoon in the Southwest Pacific Ocean (Dandonneau and Gohin, 1984; Dupouy et al., 2011).

Trichodesmium has been extensively investigated [reviewed in Capone et al. (1997); and Bergman et al. (2012)]. Yet, relatively few publications have examined the mortality and fate of these blooms that often collapse abruptly with mortality rates paralleling growth rates and biomass declines > 50 % occurring within 24 h from peak abundance (Bergman et al., 2012; Rodier and Le Borgne, 2008; Rodier and Le Borgne, 2010). Cell mortality can occur due to grazing of *Trichodesmium* by pelagic harpacticoid copepods (O'Neil, 1998) or by viral lysis (Hewson et al., 2004; Ohki, 1999). Both iron (Fe) and phosphorus (P) availability regulate N_2 fixation and production of *Trichodesmium* populations, causing a variety of stress responses when these nutrients are limited (Berman-Frank et al., 2001). Fe depletion as well as oxidative stress can also induce in *Trichodesmium* a genetically controlled programmed cell death (PCD) that occurs in both laboratory cultures and in natural populations (Bar-Zeev et al., 2013; Berman-Frank et al., 2004; Berman-Frank et al., 2007). Mortality of *Trichodesmium* via PCD is morphologically and physiologically distinct from necrotic death and triggers rapid sinking of biomass that could enhance carbon export in oligotrophic environments (Bar-Zeev et al., 2013). Sinking is due to concomitant internal cellular degradation, vacuole loss, and the increased production of extracellular polysaccharide aggregates, operationally defined as transparent exopolymeric particles (TEP) (Bar-Zeev et al., 2013; Berman-Frank et al., 2004; Berman-Frank et al., 2007).

The VAHINE project investigated the fate of newly fixed N by diazotrophs and aimed to test changes in organic matter export, following diazotroph development and mortality. For this, large (50 m^3) mesocosms were deployed in the in the New Caledonian lagoon and followed

over the course of 23 days (Bonnet et al., 2016a). Our objective during the VAHINE project was to study the involvement of PCD in the fate of natural *Trichodesmium* blooms induced in these mesocosms. While *Trichodesmium* was initially present, and conditions in the mesocosms appeared favorable, no *Trichodesmium* blooms developed within the mesocosms, yet UCYN-C did increase, allowing to meet the scientific objectives of the project (Berthelot et al., 2015; Bonnet et al., 2016a; Turk-Kubo et al., 2015). However, *Trichodesmium* developed at different phases of the experimental period outside the mesocosms (Turk-Kubo et al., 2015). Here, we investigated mortality processes in a short-lived *Trichodesmium* bloom that developed and crashed in the lagoon waters at the end of the VAHINE experiment. Using a series of microcosm incubations with collected *Trichodesmium* biomass, we elucidated the stressors and subcellular underpinning of rapid (~ 24 h) biomass demise and disappearance. Here we present, for the first time, physiological, biochemical, and metatranscriptomic evidence for nutrient-stress induced PCD in natural populations that lead to *Trichodesmium* mortality including concomitant downregulation of gas vesicle synthesis and enhanced TEP production. Such mechanisms would lead to enhanced export flux in natural blooms that also crash within 1-2 days.

2 Methods

2.1. Sampling site and sampling conditions during pre-bloom periods

Our study was performed during the VAHINE mesocosm project set 28 km off the coast of New Caledonia from 13 January 2013 (day 1) to 6 February 2013 in the New Caledonian oligotrophic lagoon (22°29.10’ S, 166° 26.90’ E). The 25 m deep sandy-bottom lagoon is generally protected from the dominant trade winds yet the waters of the lagoon are influenced by the oligotrophic oceanic waters coming into the lagoon via the Boulari Pass (Bonnet et al., 2016a). Detailed descriptions of the site selection and sampling strategy are provided elsewhere (Bonnet et al., 2016a). The lagoon water outside the mesocosms was sampled daily during the experiment and serve as ‘pre-bloom’ data. Large volume samples (50 L) were collected from 1, 6, and 12 m depths at 07:00 using a Teflon® PFA pump and PVC tubing. Samples were immediately transferred back to laboratories aboard the R/V Alis and subsampled for a suite of parameters [as described below and in Bonnet et al. (2016a)]. On day 23 at 12:00 h, we observed a large surface accumulation of *Trichodesmium* in the lagoon close to the enclosed mesocosms. This biomass accumulation (hereafter called – “bloom”)

served as the source for experiments 1 and 2 to examine the fate of *Trichodesmium* (section 2.2, Fig. S1).

2.2. Short-term incubations to assess bloom decline

Experiment 1 – *Trichodesmium* filaments and colonies were collected from the dense surface bloom (day 23, 12:00 h; designated T_0, Fig. 2a-c) using a plankton net (mesh size, 80 µm) towed through different patches of the bloom from the surface water. The total contents of the net were combined and resuspended in filtered seawater (FSW) (0.2 µm pore size), split between six identical 4.5 L Nalgene polycarbonate bottles (Fig. 2d-e), and incubated as detailed below. Based on previous experience (Berman-Frank et al., 2004), resuspension of *Trichodesmium* cells in the extremely high densities of the surface blooms (> 1 mg L^{-1} Chl *a*; Fig. 2a-c) would cause an almost immediate crash of the biomass. Consequently, we resuspended the collected biomass in FSW at ~ 1000 fold lower cell densities (150 µg L^{-1}) that resemble the cellular abundance at the edges of the slicks (Fig. 2). **Experiment 2 –** Seawater from the surface bloom was collected 5 h after the initial surface bloom was sighted (day 23, 17:00) by using a Teflon® PFA pump and PVC tubing directly filling nine 20 L polyethylene carboys gently to avoid destroying biomass. Bottles from experiments 1 and 2 were placed in on-deck incubators, filled with running seawater to maintain ambient surface temperature (~ 26 °C), and covered with neutral screening at 50 % surface irradiance levels. Water from experiment 1 was sampled every 2-4 h until the biomass collapsed (after ~ 22 h) for: Chl *a* concentration, caspase activity, 16S rRNA gene sequencing, and metatranscriptomics. Water from experiment 2 was sampled for PON, POC, NH_4^+, N_2 fixation rates, TEP production, and virus abundance (days 23-25) (Fig. S1). Prior to incubations, all incubation bottles and carboys were washed with 10 % HCl overnight and rinsed 3 times with ambient seawater.

2.3. Chlorophyll *a* concentrations

Samples for the determination of Chl *a* concentrations during pre-bloom days were collected by filtering 550 mL of seawater on GF/F filters. Filters were directly stored in liquid nitrogen. Chl *a* was extracted in methanol and measured fluorometrically (Herbland et al., 1985). During short-term experiment 1, samples for Chl *a* were collected by filtering 200 mL on GF/F filters (Whatman, Kent, UK). Chl *a* was extracted in methanol and measured

spectrophotometrically (664 and 750 nm; CARY100, Varian, Santa Clara, CA, USA) according to Tandeau de Marsac and Houmard (1988).

2.4. Particulate organic carbon (POC) and nitrogen (PON)

Detailed POC and PON analyses are described in Berthelot et al. (2015). POC samples were collected by filtering 2.3 L of seawater through pre-combusted (450 °C, 4 h) GF/F filter and determined using the combustion method (Strickland and Parsons, 1972) on an EA 2400 CHN analyzer. Samples for PON concentrations were collected by filtering 1.2 L of water on pre-combusted (450 °C, 4 h) and acid washed (HCl, 10 %) GF/F filters and analyzed according to the wet oxidation protocol described in Pujo-Pay and Raimbault (1994) with a precision of 0.06 µmol L^{-1}.

2.5. N_2 fixation rates and NH_4^+ concentrations

N_2-fixation rate measurements used in experiment 2 are described in detail in (Berthelot et al., 2015). Samples were collected at 17:00 in 4.5 L polycarbonate bottles and amended with $^{15}N_2$-enriched seawater, within an hour of biomass collection, according to the protocol developed by Mohr et al. (2010) and Rahav et al. (2013). Briefly, seawater was degassed through a degassing membrane (Membrana, Minimodule®, flow rate fixed at 450 mL min^{-1}) connected to a vacuum pump. Degassed seawater was amended with 1 mL of $^{15}N_2$ (98.9 % atom ^{15}N, Cambridge Isotopes) per 100 mL. The bottle was shaken vigorously and incubated overnight at 3 bars to promote $^{15}N_2$ dissolution. Incubation bottles were amended with 1:20 (vol:vol) of $^{15}N_2$-enriched seawater, closed without headspace with silicone septum caps, and incubated for 24 h under *in situ*-simulated conditions in on-deck incubators (described above). 2.2 L from each experimental bottle was filtered under low vacuum pressure (< 100 mm Hg) onto a pre-combusted (450 °C, 4 h) GF/F filter (25 mm diameter, 0.7 µm nominal porosity). The filters were stored at -20 °C and dried for 24 h at 60 °C before mass spectrometric analysis. PON content and PON ^{15}N enrichments were determined using a Delta plus Thermo Fisher Scientific isotope ratio mass spectrometer (Bremen, Germany) coupled with an elemental analyzer (Flash EA, Thermo Fisher Scientific). N_2-fixation rates were calculated according to the equations detailed in Montoya et al. (1996). We assumed significant rates when the ^{15}N enrichment of the PON was higher than three times the standard deviation obtained from T_0

samples. The ^{15}N batch did not indicate that our results were overestimated by contamination of the spike solution (Berthelot et al. 2015).

Samples for NH_4^+ were collected in 40 mL glass vials and analyzed by the fluorescence method according to Holmes et al. (1999), using a Trilogy fluorometer (Turner Design).

2.6. Transparent exopolymeric particles (TEP)

Water samples (100 mL) were gently (< 150 mbar) filtered through 0.45 µm polycarbonate filter (GE Water & Process Technologies). Filters were then stained with a solution of 0.02 % Alcian blue (AB), 0.06 % acetic acid (pH of 2.5), and the excess dye was removed by a quick deionized water rinse. Filters were then immersed in sulfuric acid (80 %) for 2 h, and the absorbance (787 nm) was measured spectrophotometrically (CARY 100, Varian). AB was calibrated using a purified polysaccharide gum xanthan (GX) (Passow and Alldredge, 1995). TEP concentrations (µg GX equivalents L^{-1}) were measured according to (Passow and Alldredge, 1995)**.**

2.7. Virus abundance

Total seawater (1 mL) was fixed with 0.5 % glutaraldehyde and snap frozen in liquid N_2 until processed. Flow cytometry was conducted using an Influx Model 209S Mariner flow cytometer and high-speed cell sorter equipped with a 488 nm 200 mW blue laser, 4 way sort module, 2 scatter, 2 polarized and 4 fluorescence detectors (BD Biosciences). Viral abundance was determined by staining fixed seawater samples with SYBR Gold (Life Technologies) and measurements of green fluorescence (520 nm**,** 40 nm band pass). Samples were thawed, diluted 25-fold in 0.22 µm-filtered Tris/EDTA (TE) buffer (pH 8), stained with SYBR Gold (0.5 - 1X final concentration), incubated for 10 min at 80°C in the dark, cooled to RT for 5 min, and mixed thoroughly by vortexing prior to counting on the Influx (Brussaard, 2003). Viral abundance was analyzed using a pressure differential (between sheath and sample fluid) of 0.7, resulting in a low flow rate for higher event rates of virus like particles counts.

2.8. Caspase activity

Biomass was collected on 25 mm, 5 µm pore-size polycarbonate filters and resuspended in 0.6-1 mL Lauber buffer [50 mM HEPES (pH 7.3), 100 mM NaCl, 10 % sucrose, 0.1 % 3-(3-cholamidopropyl)-dimethylammonio-1-propanesulfonate, and 10 mM dithiothreitol] and sonicated on ice (four cycles of 30 seconds each) using an ultra-cell disruptor (Sonic Dismembrator, Fisher Scientific, Waltham, MA, USA). Cell extracts were centrifuged (10,000

x *g*, 2 min, room temperature) and supernatant was collected for caspase biochemical activity. Caspase-specific activity was determined by measuring the kinetics of cleavage for the canonical fluorogenic caspase substrate (Z-IETD-AFC) at a 50 mM final concentration (using Ex 400 nm and emission 505 nm; Synergy4 BioTek, Winooski, VT, USA), as previously described in Bar-Zeev et al. (2013). Fluorescence was converted to a normalized substrate cleavage rate using an AFC standard (Sigma) and normalized to total protein concentrations obtained from the same samples. Total protein concentrations were determined by Pierce™ BCA Protein Assay Kit (Thermo Scientific product #23225).

2.9. 16S rRNA gene sequencing and data analyses

Bacterial community diversity was analyzed by deep sequencing of the 16S rRNA gene in samples from two replicate bottles from experiment 1 (see section 1.2) at three time points each. Seawater samples were filtered on 25 mm, 5 µm pore-size Supor filters (Pall Gelman Inc., Ann Arbor, Michigan), snap frozen in liquid nitrogen, and stored at -80 °C for later extraction. Community genomic DNA was isolated from the filters using a phenol–chloroform extraction method modified according to Massana et al. (1997). The 16S rRNA genes within community genomic DNA were initially amplified with conserved bacterial primers 27F and 1100R (Dowd et al., 2008) using a high fidelity polymerase (Phusion DNA polymerase, Thermo Scientific) with an initial denaturation step of 95 ºC for 3 min followed by 20 cycles of 95 ºC for 30 sec, 55 ºC for 30 sec, and 72 ºC for 45 sec. A secondary PCR (same conditions) was performed for next-generation sequencing by using customized fusion primers with different tag sequences. The tags were attached to the 27F primer and to the 338R primer (Hamady et al., 2008) to obtain 340 bp fragments suitable for IonTorrent analysis. The use of nested PCR was used to minimize inclusion of false sequences into the sequenced material (Dowd et al., 2008). After secondary PCR, all amplicon products were purified using Ampure magnetic purification beads (Agencourt Bio- science Corporation, MA, USA) to exclude primer-dimers. The amplicons were sequenced at the Bar-Ilan Sequencing Center, using an Ion Torrent™ (Life Technologies, USA).

The adapter-clipped sequences were processed using tools and scripts from the UPARSE pipeline (Edgar, 2013). Reads from all samples were pooled for OTU calling. Reads were de-multiplexed, primers and barcodes stripped using the script *fastq_strip_barcode_relabel.py*, leaving 42747 raw reads altogether for six samples. As suggested for OTU calling from single-end amplicon sequences (Edgar, 2013), sequences (mostly between 280 nt and 300 nt)

were trimmed to a fixed length of 280 nt, and shorter sequences were discarded (26740 trimmed raw reads remaining). For OTU clustering, trimmed raw reads were quality filtered using the *–fastq_filter* command with a maximum expected error rate (*-fastq_maxee*) of 2 (21590 reads remaining), clustered into unicals (100 % identity) and the unicals sorted by weight (number of sequences in the cluster). OTU clustering with an identity threshold of 0.98 was done using the *-cluster_otus* command on sorted unicals, with built-in chimera filtering. To infer OTU abundances for each individual sample, the trimmed raw reads per sample (after a more relaxed quality filtering with *-fastq_maxee* 5) were mapped back to these OTUs with *-usearch_global* and a minimum identity of 98 %. For taxonomic classification, OTUs were submitted to https://www.arb-silva.de/ngs/ and classified using the SINA aligner v1.2.10 and database release SSU 123 (Quast et al., 2013). Sequences having a (*BLAST alignment coverage + alignment identity*)/2 < 93 % were considered as unclassified and assigned to the virtual group "No Relative" (5.58 % of OTUs).

2.10. RNA extraction and metatranscriptome sequencing

Metatranscriptomic sequencing was performed for three time points: peak surface accumulation of the bloom ($T_{0,}$ 12:00), 8 h (T_8 22:00), and 22 h (T_{22} 10:00) after T_0. Cells on polycarbonate filters were resuspended in 1 mL PGTX [for 100 mL final volume: phenol (39.6 g), glycerol (6.9 mL), 8-hydroxyquinoline (0.1 g), EDTA (0.58 g), sodium acetate (0.8 g), guanidine thiocyanate (9.5 g), guanidine hydrochloride (4.6 g), Triton X-100 (2 mL)] (Pinto et al., 2009), and 250 µl glass beads (diameter 0.1 – 0.25 mm). and sonicated on a cell disruptor (Precellys, Peqlab, Germany) for 3 x 15 s at 6500 rpm. Tubes were placed on ice between each 15 s interval. RNA was extracted by adding 0.7 mL chloroform and subsequent phase separation. RNA was precipitated from the aqueous phase using 3 volumes of isopropanol at -20 °C overnight. Residual DNA was removed using the Turbo DNA-free Kit (Ambion) after the manufacturer's instructions, but adding additional 1 µl of DNase after 30 min of incubation and incubating another 30 min. RNA was purified using Clean & Concentrator 5 columns (C&C 5) (Zymo Research, Freiburg, Germany). The pure RNA was treated with Ribo-Zero rRNA Removal Kit (Bacteria) (Epicentre, Madison, USA) and purified again with C&C 5. DNA contamination was tested and confirmed negative with a 40 cycle PCR using cyanobacteria-specific 16S primers.

For removal of tRNAs and small fragments, the RNA was purified with the Agencourt RNAClean XP kit (Beckman Coulter Genomics, Danvers, USA). First-strand cDNA synthesis

for T_8 and T_{22} samples was primed with a N6 randomized primer, after which the cDNAs were fragmented by ultrasound (4 pulses of 30 sec at 4 °C). Illumina TruSeq sequencing adapters were ligated in a strand-specific way to the 5' and 3' ends and the resulting cDNAs were PCR-amplified to about 10-20 ng μL^{-1} using a high fidelity DNA polymerase. Randomly-primed cDNA for T_0 samples was prepared using purified RNA without fragmentation followed by ligation of Illumina TruSeq sequencing adapters to the 5' and 3' ends and fragmentation of cDNA > ~700 bp with ultrasound (4 pulses of 30 sec at 4°C; targeting only cDNA > 700 nt). After repairing ends, fragments were dA-tailed and Illumina TruSeq sequencing adapters were ligated again to the 5' and 3' ends of the cDNA and re-amplified. Consequently, a small fraction of the T_0 reads was not strand-specific. All cDNAs were purified using the Agencourt AMPure XP kit (Beckman Coulter Genomics, Danvers, USA) and 2 x 150 nt paired-end sequences generated with an Illumina NextSeq500 sequencer by a commercial provider (vertis AG, Freising, Germany).

2.11. Bioinformatics processing and analysis of metatranscriptome data

To remove adapters, perform quality trimming, and set a minimal length cutoff, raw fastq reads were processed with Cutadapt version 1.8.1 (Martin, 2011) in paired-end mode with a minimum adapter sequence overlap of 10 nt (-O 10), an allowed error rate of 20 % (-e 0.2) in the adapter sequence alignment, and a minimum base quality of 20. To remove residual ribosomal RNA reads, the fastq files were further processed with SortMeRNA version 1.8 (Kopylova et al., 2012) with the accompanying standard databases in paired end mode, resulting in 9,469,339 non-ribosomal reads for T_0, 22,407,194 for T_8, and 18,550,250 for T_{22}. The fastq files with all non-ribosomal forward-reads were used for mapping against the *Trichodesmium erythraeum* IMS101 genome with Bowtie2 (Langmead and Salzberg, 2012) in *very-sensitive-local* mode. This resulted in 51.9 % of T_0, 5.1 % of T_8, and 3.3 % of T_{22} reads mapped. Reads were counted per CDS feature as annotated in the genome of *Trichodesmium erythraeum* (NC_008312.1) using htseq-count version 0.6.0 (Anders et al., 2014) and a count table generated with all read counts from T_0, T_8, and T_{22}.

For detection of differentially expressed genes from T_0 to T_8 and T_8 to T_{22}, the count table was processed with the statistical tool "Analysis of Sequence Counts" (ASC) (Wu et al., 2010). This tool is specifically designed to account for missing replicates by employing a model of biological variation of gene expression (Wu et al., 2010). The posterior probabilities (P) of a gene being > 2-fold differentially expressed (user specified threshold) between any two

samples is calculated using an empirical Bayesian analysis algorithm and an internal normalization step. Differential expression of genes was defined as significant if $P > 0.98$.

3 Results

3.1. Setting the scene – *Trichodesmium* bloom development and bloom within the lagoon.

Trichodesmium were present as part of the *in-situ* community in the lagoon at the outset of the VAHINE experiment. (Bonnet et al., 2015; Turk-Kubo et al., 2015). In the lagoon water, temperatures were high (> 25 °C) and typical oligotrophic conditions of austral summer prevailed. For the first 20 days of the experiment low abundance and biomass was measured for primary and secondary production and specifically for diazotrophic populations (Fig. 1). Total PON and POC in the lagoon fluctuated in the first 20 days of the VAHINE experiment with values ranging between 0.6-1.1 µmol L^{-1} and 5-11 respectively. On the morning of day 23, values were 0.9 and 9.3 µmol L^{-1} PON and POC, respectively (Fig. 1c-d). The total Chl *a* concentrations ranged between 0.18-0.26 µg L^{-1} from days 1-20 (Fig. 1a). The increase in Chl *a* concentrations reflect the composite signature of the total phototrophic community [detailed in (Leblanc et al., 2016; Van Wambeke et al., 2015)] and is not specific to *Trichodesmium* biomass. Low abundances of *Trichodesmium* were measured in the lagoon waters throughout the first three weeks of the project (Turk-Kubo et al., 2015), with *Trichodesmium*-associated 16S counts ranging from 0.1 to 0.4 % of the total number of 16S tags (Pfreundt et al., 2016). During the first eight days of sampling, *Trichodesmium* abundance as measured by *nifH* gene real-time PCR ranged from 3.4×10^2-6.5×10^3 *nifH* copies L^{-1}. By days 14 and 16, *Trichodesmium* accounted for 15 % of the total diazotroph population (with 1.1-1.5×10^4 *nifH* copies L^{-1}) increasing by day 22 to 42 % of the diazotroph population (1.4×10^5 *nifH* copies L^{-1}) (Turk-Kubo et al., 2015). By the morning of day 23, Chl *a* increased to 0.39 µg L^{-1} in the upper 1 m depth (Fig. 1a), yet *Trichodesmium* was still not visually observed at this time as a bloom on the sea surface. Phycoerythrin concentrations fluctuated between 0.1-0.4 µg L^{-1} during days 1-14 and then increased to a maximal peak of > 0.8 µg L^{-1} on day 21 with values ~ 0.5 µg L^{-1}on day 23 reflecting both the doubling in *Synechococcus* biomass (days 15-23) as well as increasing *Trichodesmium* (days 21-23) (Leblanc et al., 2016). N_2 fixation rates in the lagoon waters ranged between 0.09 -1.2 nmol N L^{-1} h^{-1} during the pre-bloom period (Fig. 1c) and on the morning of day 23 measured 0.5 nmol L^{-1} h^{-1} (Fig. 1c).

Zooplankton populations in the lagoon fluctuated around 5000 individuals m^{-3} and increased from day 9 to 16 to peak at ~ 14000 individuals m^{-3} (Hunt et al., 2016). From day 16 to day 23 the total zooplankton population declined to ~ 8000 individuals m^{-3} with harpacticoid copepods including grazers of *Trichodesmium* (*Macrosetella gracilis*, *Miracia efferata*, and *Oculosetella gracilis)* comprising < 1.5 % of total zooplankton community in the lagoon (Hunt et al., 2016). Virus like particles (VLP) ranged from 1-6 x 10^6 mL^{-1} throughout the first 22 days of the VAHINE experiment and displayed a ~ 2-4 day oscillation (i.e., increasing for 2 days, then declining for the next 3 days, etc.) with mean values of 3.8 x 10^6 mL^{-1} (Fig. 1b). VLP counts in surface waters on day 23 were 1.8 x 10^6 mL^{-1} (Fig. 1b), just prior to the appearance of the *Trichodesmium* surface bloom. VLPs did not show any distinct correlations with total biomass indices such as PON and POC during the pre-bloom sampling (Fig. 1b-d).

Depth-averaged dissolved inorganic phosphorus (DIP) concentrations in the lagoon waters were low at 0.039 ± 0.001 µM, with a relatively stable DIP turnover time (T_{DIP}) of 1.8 ± 0.7 d for the first 15 days, that declined to 0.5 ± 0.7 by day 23 (Berthelot et al., 2015). Alkaline phosphatase activity (APA), which hydrolyzes inorganic phosphate from organic phosphorus, increased ~ 3 fold, from 1.8 ± 0.7 (average of days 1-4) to 5.0 ± 1.4 nmole L^{-1} h^{-1} (average of days 19-23) (Van Wambeke et al., 2015) demonstrating a response in metabolic activity related to P acquisition for the microbial community probably related to the decreasing availability of DIP in the lagoon waters.

On day 23 (February 4) of the VAHINE measurements, dense surface accumulations of *Trichodesmium* were observed at midday (12:00 h) (Fig. 2a-c). Ambient air temperatures (~ 25 °C) increased to over 26 ºC and the winds decreased to < 5 knots. These accumulations (hereafter blooms) appeared in the typical "slick" formations of dense biomass in ribbons visible on the surface seawater and spread out over tens of meters in the lagoon water outside the mesocosms (Fig. 2a-c). *Trichodesmium* abundance in these patches was extremely variable with Chl *a* concentrations exceeding 5 mg L^{-1} within dense patches and trichome abundance > 10,000 trichomes mL. These surface accumulations were visible and sampled again 5 h later (experiment 2), yet by the next morning, no such slicks or patches of dense biomass were observed or measured in the lagoon. The disappearance of the *Trichodesmium* in the lagoon water whether by drifting away, sinking to depth, or any other factor, prevented further investigation of these populations.

3.2. Investigating *Trichodesmium* mortality in experimental microcosms.

3.2.1 Changes in *Trichodesmium* biomass and associated microbial communities.

The spatially patchy nature of *Trichodesmium* blooms in the lagoon (Fig. 2a-c), and the rapid temporal modifications in water-column abundance of filaments and colonies probably induced (primarily) by physical drivers (turbulence and wind-stress), complicate *in-situ* sampling when targeting changes in specific biomass. To overcome this, we collected *Trichodesmium* populations from the surface midday bloom and examined the physiological, biochemical, and genetic changes occurring with time until the biomass crashed ~ 24 h (see methods section 2.2) (Fig. 2 and Fig. 3). In these enclosed microcosms, *Trichodesmium* 16S copies comprised > 90 % of total copies (Fig. 3) enabling the use Chl *a* to follow changes in its biomass (Fig. 2f). Maximal Chl *a* concentrations in the incubations (> 150 ± 80 µg L^{-1}; n=6) were measured at the start of the incubation soon after the biomass collection and resuspension in FSW. These *Trichodesmium* populations collapsed swiftly over the next day with Chl *a* concentrations declining to 24 µg L^{-1} and 11 µg L^{-1} Chl *a* after 10 and 22 h, respectively (Fig. 2f).

In experiment 1 we characterized the microbial community associated with the *Trichodesmium* biomass within the microcosms by 16S rRNA gene sequencing from two replicate bottles (experiment 1). At T_0 94 % and 93 % of the obtained 16S tags in both replicates (Fig. 3) were of the Oscillatoriales order (phylum Cyanobacteria), with 99.9 % of these sequences classified as *Trichodesmium* spp. (Fig. 3). In both replicates, the temporal decline of *Trichodesmium* biomass coincided with an increase in *Alteromonas* 16S tags, but this development temporally lagged in replicate 1 compared to replicate 2 (Fig. 3). Six hours (T_6) after the surface bloom was originally sampled (T_0), over 80 % of 16S tags from replicate 1 were characterized as *Trichodesmium*. 14 h after T_0, Alteromonadales and Vibrionales replaced *Trichodesmium* now constituting only 9 % of 16S tags (Fig. 3). In replicate 2, *Trichodesmium* declined by 80 % 6 h after T_0, with Alteromonadales and Flavobacteriales comprising the bulk of the biomass 18 hours after the start of incubations (Fig.3).

The rate of decline in *Trichodesmium* biomass within the 4.6 L microcosms paralleled that of *Trichodesmium* collected from the surface accumulations at 17:00 and incubated in 20 L carboys under ambient conditions for > 72 h (defined hereafter as experiment 2: Fig. 4). Here, *Trichodesmium* biomass decreased by > 80 % within 24 h of incubations with trichome abundance declining from ~2500 trichomes mL^{-1} at bloom collection to ~ 495 trichomes mL^{-1}

(Fig. 4a). No direct correlation was observed between the decline of *Trichodesmium* and viral populations. VLP abundance at the time of the surface bloom sampling was at a maximum of 8.2 x 10^6 mL^{-1} (Fig. 4a), decreasing to 5.7 x 10^6 mL^{-1} in the next 4 h then remaining stable throughout the crash period (within the next 42 h) averaging ~ 5 x 10^6 ± 0.7 mL^{-1} (Fig. 4a).

As *Trichodesmium* crashed in the experimental incubations, high values of NH_4^+ were measured (Fig 4b). In experiment 2, NH_4^+ increased exponentially from 73 ± 0.0004 nmol NH_4^+ L^{-1} when the surface bloom was collected and placed in the carboys (17:00 h) to 1490 ± 686 after 24 h and values > 5000 nmol L^{-1} 42 h after the incubation start (Fig. 3b). The high ammonia declined somewhat by the end of the experiment (after 72 h), yet was still high at 3494 ± 834 nmol L^{-1}. Concurrently with the high NH_4^+ concentrations, and despite the dying *Trichodesmium,* we measured an increase N_2-fixation rates. N_2-fixation rose from 1.5 nmol N L^{-1} h^{-1} at T_0 to 3.5 ± 2.8 nmol N L^{-1} h^{-1} 8 h after incubations began and 11.7 ± 3.4 nmol N L^{-1} 24 h later (Fig 4b). These high values represent other diazotrophs including UCYN-types and diatom-diazotroph associations that flourished after the *Trichodesmium* biomass had declined in the carboys (Bonnet et al. 2016b; Turk-Kubo personal communication). POC and PON, representing the fraction of C and N incorporated into biomass, ranged between 5.2-11.2 µmol C L^{-1} and 0.6-1.1 µmol N L^{-1} during pre-bloom periods (Fig. 1b) and 12.6 ± 4.6 µmol C L^{-1} and 1.3 ± 0.5 µmol N L^{-1} when the surface bloom was sampled (Fig. 4b-c). 24 hours after collection of bloom biomass POC increased ~ 6-fold to 63.2 ± 15 µmol C L^{-1} and PON increased 10-fold to 10 ± 3.3 µmol N L^{-1} (Fig. 4b-c). After 72 h, total POC was 62 ± 4 µmol C L^{-1} (Fig. 4c) and PON increased to 14.1 ± 6 µmol N L^{-1} (Fig. 4b).

Organic carbon in the form of TEP is secreted when *Trichodesmium* is stressed and undergoing PCD (Bar-Zeev et al., 2013; Berman-Frank et al., 2004). TEP concentrations in the lagoon waters during the pre-bloom period (first 20 days) fluctuated around ~ 350 µg gum xanthan (GX) L^{-1} (Fig. 1d) that increased to ~ 500 µg GX L^{-1} on day 22 (Fig. 1d). During the time of biomass collection from the surface bloom TEP concentration exceeded 700 µg GX L^{-1} (Fig. 4c). After biomass enclosure (experiment 2) TEP concentrations declined to 420 ± 35 µg GX L^{-1} and subsequently to 180 ± 25 µg GX L^{-1} 42 h and 72 h after T_0 (Fig. 4c).

3.2.2. Genetic responses of stressed *Trichodesmium*

Metatranscriptomic analyses of the *Trichodesmium* biomass were conducted in samples from experiment 1, at T_0, T_8, and T_{22} (Fig. S1). We examined differential expression during this period by investigating a manually curated gene suite including specific pathways involved in

P and Fe uptake and assimilation, PCD, or gas vesicle synthesis. Genes involved in the acquisition and transport of inorganic and organic P sources were upregulated, concomitant with biomass demise; significantly higher expression levels were evident at T_8 and T_{22} compared to T_0 (Table S1). Abundance of alkaline phosphatase transcripts, encoded by the *phoA* gene (Orchard et al., 2003), increased significantly (~ 5 fold) from T_0 to T_{22} (Fig. 5a). The transcript abundance of phosphonate transporters and C-P lyase genes (*phnC, phnD, phnE, phnH, phnI, phnL* and *phnM*) increased significantly (5-12 fold) between T_0 and both T_8 and T_{22} (Fig. 5a, Table S1). Of the phosphite uptake genes, only *ptxA* involved in the phosphite (reduced inorganic phosphorus compound) uptake system, and recently found to operate in *Trichodesmium* (Martínez et al., 2012; Polyviou et al., 2015) was significantly upregulated at both T_8 and T_{22} compared to T_0 (4.5 and 7 fold change respectively). The two additional genes involved in phosphite uptake, *ptxB* and *ptxC*, did not change significantly, as *Trichodesmium* biomass crashed (Fig. 5a).

Fe limitation induces PCD in *Trichodesmium* (Berman-Frank et al., 2004; Berman-Frank et al., 2007) we therefore examined genetic markers of Fe stress. At the time of surface bloom sampling (experiment 1, T_0), Fe stress was indicated by higher differential expression of several genes. The *isiB* gene encodes flavodoxin and serves as a common diagnostic indicator of Fe stress in *Trichodesmium*, since it may substitute for Fe-S containing ferredoxin (Bar-Zeev et al., 2013; Chappell and Webb, 2010). Transcripts of *isiB* were significantly higher at T_0 (3-fold) than at T_8 and T_{22} (Fig. 5b, Table S1). The chlorophyll-binding protein IsiA is induced in cyanobacterial species under Fe or oxidative stress to prevent oxidative damage (Laudenbach and Straus, 1988). Here *isiA* transcripts increased 2- and 3- fold from T_0 to T_8 and T_{22}, respectively (Fig. 5b, Table S1). The Fe transporter gene *idiA* showed a transient higher transcript accumulation only at T_8. As the health of *Trichodesmium* declined, transcripts of the Fe-storage protein ferritin (*Dps*) decreased by > 70 % at T_{22} (Fig. 5b, Table S1)

3.2.3. PCD-induced demise.

Our earlier work demonstrating PCD in *Trichodesmium* allowed us to utilize two independent biomarkers to investigate PCD induction during *Trichodesmium* demise, namely changes in catalytic rates of caspase-specific activity (Berman-Frank et al., 2004; Berman-Frank et al., 2007) and levels of metacaspase transcript expression (Bar-Zeev et al., 2013). When the surface bloom was sampled (experiment 1, T_0), protein normalized caspase-specific activity

was 0.23 ± 0.2 pmol mg protein^{-1} min^{-1} (Fig. 6a). After a slight decline in the first 2 h, caspase activity increased throughout the experiment with 10 fold higher values (2.9 ± 1.5 pmol L^{-1} mg protein^{-1} min^{-1}) obtained over the next 22 h as the bloom crashed (Fig. 6a).

We followed transcript abundance over the demise period for the 12 identified metacaspase genes in *Trichodesmium* [(Asplund-Samuelsson et al., 2012; Asplund-Samuelsson, 2015; Berman-Frank et al., 2004)]; *TeMC1* (Tery_2077), *TeMC2* (Tery_2689), *TeMC3* (Tery_3869), *TeMC4* (Tery_2471), *TeMC5* (Tery_2760), *TeMC6* (Tery_2058), *TeMC7* (Tery_1841), *TeMC8* (Tery_0382), *TeMC9* (Tery_4625), *TeMC10* (Tery_2624), *TeMC11* (Tery_2158), and *TeMC12* (Tery_2963)] (Fig. 6b, Table S1). A subset of these genes was previously implicated in PCD of *Trichodesmium* cultures in response to Fe and light stress (Bar-Zeev et al., 2013; Berman-Frank et al., 2004; Bidle, 2015). Here, we interrogated the entire suite of metacaspases in natural *Trichodesmium* populations. As the biomass crashed from T_0 to T_{22}, 7 out of 12 metacaspases (TeMC1, TeMC3, TeMC4, TeMC7, TeMC8, TeMC9, and TeMC11) were significantly upregulated 8 and 22 h after T_0 (Fig. 6b). For these genes, transcript abundance increased 2.3- to 5.3-fold 8 h after T_0 and 3.5-6.2-fold 22 h after T_0 (Fig. 6b, Table S1) TeMC5 and TeMC10 transcripts increased significantly after 22 h by 2.9- and 3.2 fold, respectively. TeMC6 was upregulated 2.9-fold after 8 h. TeMC2 transcripts did not significantly change over time. We did not detect any expression of *TeMC12* throughout the experiment.

Export flux can be enhanced by PCD-induced sinking (Bar-Zeev et al., 2013) as PCD in *Trichodesmium* results in degradation of internal components, especially gas vesicles that are required for buoyancy (Berman-Frank et al., 2004). Although we did not measure changes in buoyancy itself, we observed rapid sinking of the *Trichodesmium* biomass in the bottles and carboys. The metatranscriptomic analyses demonstrated that, excluding one copy of *gvpL/gvpF*, encoding a gas vesicle synthesis protein, gas vesicle protein *(gvp)* genes involved in gas-vesicle formation *(gvpA, gvpN, gcpK, gvpG and gvpL/gcpF)* were all significantly downregulated relative to T_0 (Fig. 7, Table S1).

4 Discussion

4.1. Mortality processes of *Trichodesmium* – incubation results.

4.1.1 Grazer and virus influence.

Our microcosm incubations allowed us to specifically focus on the loss factors and show the involvement of biotic and abiotic stressors in inducing PCD and mechanistically impacting the

demise and fate of a natural *Trichodesmium* bloom. We appreciate that the enclosure of the biomass in bottles and carboys may accelerate the processes occurring in the natural lagoon setting. Yet, the published rates of *Trichodesmium* mortality from field studies (Rodier and Le Borgne, 2010) indicate that these can parallel our loss rates with natural bloom demise occurring 24-48 h after peak of biomass.

We focused initially on biotic factors that could impact the incubated *Trichodesmium* biomass. The low number of harpacticoid zooplankton specific to *Trichodesmium* (O'Neil and Roman, 1994; O'Neil, 1998) in the lagoon (Hunt et al., 2016) and especially those in the bottles (personal observation) refutes the hypothesis that grazing caused the massive mortality of *Trichodesmium* biomass in our experimental incubations.

Viruses have been increasingly invoked as key agents terminating phytoplankton blooms (Brussaard et al., 2005; Jacquet et al., 2002; Lehahn et al., 2014; Tarutani et al., 2000; Vardi et al., 2012). In *Trichodesmium*, phages have been implicated in bloom crashes, but this mechanism has yet to be unequivocally proven (Hewson et al., 2004; Ohki, 1999); indeed, no specific *Trichodesmium* phage has been isolated or characterized to date (Brown et al., 2013). Here, total VLP abundance was highest at the time of sampling from the surface *Trichodesmium* bloom and at the start of the incubation at ~ 8 x 10^6 VLPs mL^{-1} it actually declined 2 fold in the first eight hours of incubation before increasing over the next 32 h (Fig. 4a). While our method of analysis cannot distinguish between phages infecting *Trichodesmium* from those infecting other marine bacteria, it argues against a massive, phage-induced lytic event of *Trichodesmium*. Such an event would have yielded a notable burst of VLPs upon bloom crash, especially considering the high *Trichodesmium* biomass observed. The coincidence between the maximal abundance of VLPs and highest *Trichodesmium* biomass is counter to viruses serving as the mechanism of mortality in our incubation experiments. Nonetheless, virus infection itself may be a stimulant for community N_2 fixation perhaps by releasing key nutrients (i.e., P or Fe) upon lysis of surrounding microbes (Weitz and Wilhelm, 2012). Although we did not characterize them here, it is indeed possible that *Trichodesmium*-specific phages were present in our incubation experiments and they may have exerted additional physiological stress on resident populations, facilitating PCD induction. Virus infection increases the cellular production of reactive oxygen species (ROS) (Evans et al., 2006; Vardi et al., 2012), which in turn can stimulate PCD in algal cells (Berman-Frank et al., 2004; Bidle, 2015; Thamatrakoln et al., 2012). Viral attack can also directly trigger PCD as part of an antiviral defense system activated to limit virus production

and prevent massive viral infection (Bidle and Falkowski, 2004; Bidle, 2015; Georgiou et al., 1998).

4.1.2 Stressors impacting mortality.

Nutrient stress can be acute or chronic to which organisms may acclimate on different time scales. Thus, for example, the consistently low DIP concentrations measured in the lagoon during the 22 days preceding the *Trichodesmium* surface bloom probably enabled acclimation responses such as induction of APA and other P acquisition systems. *Trichodesmium* has the ability to obtain P via inorganic and organic sources including methylphosphonate, ethylphosphonate, 2-aminoethylphosphonate (Beversdorf et al., 2010; Dyhrman et al., 2006), and via a phosphite uptake system (PtxABC) that accesses P via the reduced inorganic compound phosphite (Martínez et al., 2012; Polyviou et al., 2015). Our metatranscriptomic data demonstrated upregulated expression of genes related to all three of these uptake systems (DIP, phosphonates, phosphites) 8 and 22 h after incubation began, accompanying biomass demise (Fig. 5a). This included one gene for phosphite uptake (*ptx*A) and several genes from the phosphonate uptake operon (*phn*DCEEGHIJKLM) (Hove-Jensen et al., 2014). Upregulated expression of *phnD, phnC, phnE, phnH, phnI, phnJ, phnK, phnL* and *phnM* occurred as the *Trichodesmium* biomass crashed (Fig. 5a, Table S1), consistent with previous results demonstrating that *phnD* and *phnJ* expression levels increased during DIP depletion (Hove-Jensen et al., 2014). It is likely that during bloom demise, the C-P lyase pathway of remaining living cells was induced when DIP sources were extremely low, while POP and DOP increased along with the decaying organic matter. The ability to use phosphonates or phosphites as a P source can provide a competitive advantage for phytoplankton and bacteria in P-depleted waters (Coleman and Chisholm, 2010; Martinez et al., 2010). Thus, it is puzzling why dying cells would upregulate *phn* genes or *phoA* transcripts after 22 h incubation (Fig. 5a). A more detailed temporal resolution of the metatranscriptomic analyses may elucidate the expression dynamics of these genes and their regulating factors. Alternatively, in PCD-induced populations, a small percentage remains viable and resistant as either cysts (Vardi et al., 1999) or hormogonia (Berman-Frank et al., 2004) that can serve as the inoculum for future blooms. It is plausible that the observed upregulation signal was attributable to these sub-populations.

The concentrations of dissolved and bioavailable Fe were not measured in the lagoon water during the experimental period as Fe is typically replete in the lagoon (Jacquet et al., 2006). However, even in Fe-replete environments such as the New Caledonian lagoon, dense patches

of cyanobacterial or algal biomass can deplete available resources and cause limited micro-environments (Shaked, 2002). We obtained evidence for Fe stress using several proxy genes demonstrating that enhanced cellular Fe demand occurred during the bloom crash (Table S1). *Trichodesmium*'s strategies of obtaining and maintaining sufficient Fe involves genes such as *isiB. isiB* was highly expressed when biomass accumulated on the surface waters, indicative for higher Fe demand at this biomass load (Bar-Zeev et al., 2013; Chappell and Webb, 2010). Transcripts for chlorophyll-binding, Fe-stress-induced protein A (*IsiA*) increased (albeit not significantly) 3-fold over 22 h of bloom demise (Fig. 5b, Table S1). In many cyanobacteria, *isiA* expression is stimulated under Fe stress (Laudenbach and Straus, 1988) and oxidative stress (Jeanjean et al., 2003) and functions to prevent high-light induced oxidative damage by increasing cyclic electron flow around the photosynthetic reaction center photosystem I (Havaux et al., 2005; Latifi et al., 2005; Michel and Pistorius, 2004). Dense surface blooms of *Trichodesmium* are exposed to high irradiance (on day 23 average PAR was 3000 μmol photons m^{-2} s^{-1}). It is possible that high Fe demand combined with the oxidative stress of the high irradiance induced the higher expression of *isiA* (Fig. 5b). As cell density and associated self-shading of *Trichodesmium* filaments decreased during bloom crash, light-induced oxidative stress is likely the principal driver for elevated *isiA* expression.

The gene *idiA* is another environmental Fe stress biomarker that allows acquisition and transfer of Fe through the periplasm into the cytoplasm (Chappell and Webb, 2010). In our incubation, upregulated expression of *idiA* (an ABC Fe^{+3} transporter) was evident after 8 h. This is consistent with increasing Fe-limitation, as *Trichodesmium* abundance (measured via 16S rRNA gene sequencing) was still high at T_6 (after 6 h of incubations) (replicate 1). These findings are consistent with proteomics analyses from deplete iron (0 μM Fe) *Trichodesmium* cultures which revealed an increase in IdiA protein expression (Snow et al., 2015). Lastly, our metatranscriptomic data highlighted a reduction in Fe storage and utilization, as the expression of Fe-rich ferritin-like DPS proteins (Castruita et al., 2006), encoded by *dps*A, decreased ~ 5 fold by the time that most of the biomass had crashed (T_{22}) (Fig. 5b, Table S1). *dpsA* was also downregulated under Fe-replete conditions in *Synechococcus* (Mackey et al., 2015), but the downregulation observed here is more likely related to *Trichodesmium* cells dying and downregulating Fe-demanding processes such as photosynthesis and N_2 fixation.

4.1.3. Programmed cell death (PCD) and markers for increased export flux.

598 The physiological and morphological evidence of PCD in *Trichodesmium* has been previously
599 documented in both laboratory (Bar-Zeev et al., 2013; Berman-Frank et al., 2004) and
600 environmental cultures collected from surface waters around New Caledonia (Berman-Frank
601 et al., 2004). Here, we confirmed characteristic features of autocatalytic PCD in
602 *Trichodesmium* such as increased caspase-specific activity (Fig. 6a), globally enhanced
603 metacaspase expression (Fig. 6b), and decreased expression of gas vesicle maintenance (Fig.
604 7). Metatranscriptomic snapshots interrogating expression changes in all *Trichodesmium*
605 metacaspases (Fig. 6b) generally portrayed upregulated expression concomitant with biomass
606 decline. Our results are consistent with previous observations that Fe-depleted PCD-induced
607 laboratory cultures of *Trichodesmium* IMS101 had higher expression levels of *TeMC1* and
608 *TeMC9* compared to healthy Fe-replete cultures (Bar-Zeev et al., 2013; Berman-Frank et al.,
609 2004). To our knowledge, this is the first study examining expression levels of metacaspases
610 in environmental *Trichodesmium* samples during a natural bloom. 11 of the 12 annotated
611 metacaspases in *Trichodesmium* were expressed in all 3 metatranscriptomes from the surface
612 bloom. To date, no specific function has been determined for these metacaspases in
613 *Trichodesmium* other than their association with cellular stress and death. Efforts are
614 underway to elucidate the specific cellular functions, regulation, and protein interactions of
615 these *Trichodesmium* metacaspases (Pfreundt et al., 2014; Spungin et al., In prep).

616 In cultures and isolated natural populations of *Trichodesmium*, high caspase-like specific
617 activity is correlated with the initial induction stages of PCD with activity declining as the
618 biomass crashes (Bar-Zeev et al., 2013; Berman-Frank et al., 2004; Berman-Frank et al.,
619 2007). Here, caspase-like activity increased with the crashing populations of *Trichodesmium*
620 (Fig. 5a). Notably, maximal caspase activities were recorded at T_{23}, after which most
621 *Trichodesmium* biomass had collapsed. The high protein-normalized caspase-specific activity
622 may be a result of a very stressed and dying sub-population of *Trichodesmium* that had not yet
623 succumbed to PCD (Berman-Frank et al., 2004). Alternatively, the high caspase-like activity
624 may be attributed to the large population of *Altermomonas* bacteria that were associated with
625 the remaining detrital *Trichodesmium* biomass. However, currently, we are unaware of any
626 publications demonstrating high cellular caspase-specific activity in clades of γ-
627 Proteobacteria.

628 Gas vesicles are internal structures essential for maintaining buoyancy of *Trichodesmium*
629 populations in the upper surface waters enabling them to vertically migrate and respond to
630 light and nutrient requirements (Capone et al., 1997; Walsby, 1978). Mortality via PCD causes

a decline in the number and size of cellular gas vesicles in *Trichodesmium* (Berman-Frank et al., 2004) and results in an enhanced vertical flux of trichomes and colonies to depth (Bar-Zeev et al., 2013). Our metatranscriptomic data supported the subcellular divestment from gas vesicle production during bloom decline, as the expression of vesicle-related genes was downregulated (Fig. 7). In parallel, TEP production and concentration increased to > 800 µg GX L^{-1}, a 2-fold increase from pre-bloom periods (Fig. 1d and Fig. 4c). When nutrient uptake is limited, but CO_2 and light are sufficient, uncoupling occurs between photosynthesis and growth (Berman-Frank and Dubinsky, 1999), leading to increased production of excess polysaccharides, such as TEP, and corresponding with high TEP found in bloom decline phases rather than during the increase in population density (Engel, 2000; Smetacek, 1985). In earlier studies we demonstrated that PCD-induced demise in *Trichodesmium* is characterized by an increase in excreted TEP, (Berman-Frank et al., 2007) and enhanced sinking of particulate organic matter (Bar-Zeev et al., 2013). TEP itself may be positively buoyant (Azetsu-Scott and Passow, 2004), yet its stickiness causes aggregation and clumping of cells and detritus, ultimately enhancing sinking rates of large aggregates including dying *Trichodesmium* (Bar-Zeev et al., 2013).

4.1.4. Changes in microbial community with *Trichodesmium* decline.

In the incubations, other diazotrophic populations succeeded the declining *Trichodesmium* biomass as indicated by increasing N_2 fixation rates, POC, and PON (Fig. 4b). In experiment 2, based on qPCR of targeted diazotrophic phylotypes, the diazotroph community composition shifted from being dominated by *Trichodesmium* spp. and unicellular groups UCYN-A1, UCYN-A2, and UCYN-B (T0), to one dominated by diatom-diazotroph associations Het-1 and Het-2 (T_{72}) (Bonnet et al. 2016b; Turk-Kubo, personal communication). In experiment 1 heterotrophic bacteria thrived and increased in abundance as the *Trichodesmium* biomass crashed (Fig. 3).

Trichodesmium colonies host a wide diversity of microorganisms including specific epibionts, viruses, bacteria, eukaryotic microorganisms and metazoans (Hewson et al., 2009; Hmelo et al., 2012; Ohki, 1999; Paerl et al., 1989; Sheridan et al., 2002; Siddiqui et al., 1992; Zehr, 1995). Associated epibiont bacterial abundance in dilute and exponentially growing laboratory cultures of *Trichodesmium* is relatively limited (Spungin et al., 2014) compared to bloom conditions (Hewson et al., 2009; Hmelo et al., 2012). Proliferation of *Alteromonas* and other γ-Proteobacteria during biomass collapse (Fig. 3) confirms their reputation as opportunistic microorganisms (Allers et al., 2008; Hewson et al., 2009; Frydenborg et al., 2014; Pichon et

al., 2013). Such organisms can thrive on the influx of organic nutrient sources from the decaying *Trichodesmium* as we observed (Fig. 3). Furthermore, the increase of organic matter including TEP produced by the stressed *Trichodesmium* (Fig. 1d and Fig. 4c) probably stimulated growth of these copiotrophs. Moreover, as the *Trichodesmium* biomass declined in the carboys, the high concentrations of NH_4^+ (> 5000 nmol L^{-1}) (Fig. 4b) sustained both autotrophic and heterotrophic organisms (Berthelot et al., 2015; Bonnet et al., 2015; Bonnet et., 2016b). Thus, the increase in volumetric N_2 fixation and PON that was measured in the incubation bottles right after the *Trichodesmium* crash in experiment 2 (Fig 4b) probably reflects both the enhanced activity of other diazotrophs (see above and Bonnet et al. 2016b) and resistant residual *Trichodesmium* trichomes (Berman-Frank et al. 2004) with increased cell specific N_2 fixation. This scenario is consistent with the hypothesis that PCD induction and death of a fraction of the population confers favorable conditions for survival and growth of individual cells (Bidle and Falkowski, 2004).

4.2. Implications for the lagoon system and export flux.

Phytoplankton blooms and their dense surface accumulations occur under favorable physical properties of the upper ocean (e.g. temperature, mixed-layer depth, stratification) and specifically when division rates exceed loss rates derived from grazing, viral attack, and sinking or export from the mixed layer to depth (Behrenfeld, 2014). Although physical drivers such as turbulence and mixing may scatter and dilute these dense accumulations, the rapid disappearance of biomass in large sea-surface *Trichodesmium* blooms (within 1-2 d in the lagoon waters) (Rodier and Le Bourne 2010) suggests loss of biomass by other mechanisms. The lack of *Trichodesmium* developing within the VAHINE mesocosms and the spatial-temporal variability of the surface bloom in the lagoon prohibited *in-situ* sampling of the same biomass for several days and prevented conclusions regarding *in-situ* mortality rates and export flux. Furthermore, within these dense surface populations as well as in the microcosm and carboy experiments, nutrient availability was probably extremely limited due to high demand and competition (Shaked 2002). PCD induced by Fe-depletion experiments with laboratory cultures and natural populations results in rapid biomass demise typically beginning after 24 h with > 90 % of the biomass crashing 3 to 5 days after induction (Bar-Zeev et al., 2013; Berman-Frank et al., 2004; Berman-Frank et al., 2007). In similar experiments with P-depletion, *Trichodesmium* biomass did not crash rapidly. Rather, limitation induced colony formation and elongation of trichomes (Spungin et al., 2014) and the cultures could be sustained for another couple of weeks before biomass declined significantly (unpublished

data). The responses we quantified from the dying *Trichodesmium* in the carboys and bottles (Fig. 3-7) were similar to those obtained from controlled laboratory experiments where the nutrient stressors P and Fe were validated individually. However, the rapid response here probably reflects an exacerbated reaction due to the simultaneous combination of different stressors and the presence of biotic components that can compete for and utilize the organic resources (carbon, nitrogen, phosphorus) generated by the dying *Trichodesmium*. In the lagoon, production of TEP by stressed biomass combined with the degradation of gas vesicles and enhanced aggregation will cause such surface accumulations or blooms to collapse leading to rapid vertical export of newly fixed nitrogen and carbon in the ocean.

5 Conclusions and implications

We demonstrate that the rapid demise of a *Trichodesmium* surface bloom in New Caledonia, with the disappearance of > 90 % of the biomass within 24 h in 4.5 L bottle incubations, displayed cellular responses to P and Fe stress and was mediated by a suite of PCD genes. Virus infection and lysis did not appear to directly cause the massive biomass decline. Although virus infection may have modulated the cellular and genetic responses to enhance PCD-driven loss processes. Quorum sensing among epibionts (Hmelo et al., 2012; Van Mooy et al., 2012), allelopathic interactions, and the production of toxins by *Trichodesmium* (Guo and Tester, 1994; Kerbrat et al., 2010) are additional factors that could be important for a concerted response of the *Trichodesmium* population, yet we did not examine them here. Collectively, they would facilitate rapid collapse and loss of *Trichodesmium* populations, and possibly lead to enhanced vertical fluxes and export production, as previously demonstrated in PCD-induced laboratory cultures of *Trichodesmium* (Bar-Zeev et al., 2013). We posit that PCD induced demise, in response to concurrent cellular stressors, and facilitated by concerted gene regulation, is typical in natural *Trichodesmium* blooms and leads to a high export production rather than regeneration and recycling of biomass in the upper photic layers.

Author contributions

IBF, DS, and SB conceived and planned the study. DS, UP, HB, SB, WRH, KB and IBF all participated in the experimental sampling. DS, UP, WRH, HB, FN, DAR, KB, and IBF analyzed the samples and resulting data. IBF and DS wrote the manuscript with further contributions to the manuscript by UP, WRH, SB, and KB.

Acknowledgments

Funding was obtained for IBF through a collaborative grant from MOST Israel and the High Council for Science and Technology (HCST)-France, and a United States-Israel Binational Science Foundation (BSF) grant (No: 2008048) to IBF and KB. This research was partially funded by the Gordon and Betty Moore Foundation through Grant GBMF3789 to KDB. The participation of IBF, DS, UP, and WRH in the VAHINE experiment was supported by the German-Israeli Research Foundation (GIF), project number 1133-13.8/2011 to IBF and WRH, and the metatranscriptome analysis by the EU project MaCuMBA (Marine Microorganisms: Cultivation Methods for Improving their Biotechnological Applications; grant agreement no: 311975) to WRH. Funding for VAHINE Experimental project was provided by the Agence Nationale de la Recherche (ANR starting grant VAHINE ANR-13-JS06-0002), INSU-LEFE-CYBER program, GOPS, IRD and M.I.O. The authors thank the captain and crew of the R/V Alis. We acknowledge the SEOH divers service from the IRD research center of Noumea (E. Folcher, B. Bourgeois and A. Renaud) and from the Observatoire Océanologique de Villefranche-sur-mer (OOV, J.M. Grisoni) as well as the technical service of the IRD research center of Noumea for their helpful technical support. Thanks especially to E. Rahav for his assistance throughout the New Caledonia experiment and to H. Elifantz for technical assistance with the 16S sequencing and data analysis. This work is in partial fulfillment of the requirements for a PhD thesis for D. Spungin at Bar-Ilan University. We thank the three reviewers whose comments help improve the manuscript substantially

References

Allers, E., Niesner, C., Wild, C., and Pernthaler, J.: Microbes enriched in seawater after addition of coral mucus, Applied and Environmental Microbiology, 74, 3274-3278, 2008.

Anders, S., Pyl, P. T., and Huber, W.: HTSeq–A Python framework to work with high-throughput sequencing data, Bioinformatics, btu638, 2014.

760 Asplund-Samuelsson, J., Bergman, B., and Larsson, J.: Prokaryotic caspase homologs:
761 phylogenetic patterns and functional characteristics reveal considerable diversity, PLOS One,
762 7, e49888, 2012.

763 Asplund-Samuelsson, J.: The art of destruction: revealing the proteolytic capacity of bacterial
764 caspase homologs, Molecular Microbiology, 98, 1-6, 2015.

765 Azetsu-Scott, K., and Passow, U.: Ascending marine particles: Significance of transparent
766 exopolymer particles (TEP) in the upper ocean, Limnology and Oceanography, 49, 741-748,
767 2004.

768 Bar-Zeev, E., Avishay, I., Bidle, K. D., and Berman-Frank, I.: Programmed cell death in the
769 marine cyanobacterium *Trichodesmium* mediates carbon and nitrogen export, The ISME
770 Journal, 7, 2340-2348, 2013.

771 Behrenfeld, M. J.: Climate-mediated dance of the plankton, Nature Climate Change, 4, 880-
772 887, 2014.

773 Bergman, B., Sandh, G., Lin, S., Larsson, J., and Carpenter, E. J.: *Trichodesmium* - a
774 widespread marine cyanobacterium with unusual nitrogen fixation properties, FEMS
775 Microbiology Reviews, 1-17, 10.1111/j.1574-6976.2012.00352.x., 2012.

776 Berman-Frank, I., and Dubinsky, Z.: Balanced growth in aquatic plants: Myth or reality?
777 Phytoplankton use the imbalance between carbon assimilation and biomass production to their
778 strategic advantage, Bioscience, 49, 29-37, 1999.

779 Berman-Frank, I., Cullen, J. T., Shaked, Y., Sherrell, R. M., and Falkowski, P. G.: Iron
780 availability, cellular iron quotas, and nitrogen fixation in *Trichodesmium*, Limnology and
781 Oceanography, 46, 1249-1260, 2001.

782 Berman-Frank, I., Bidle, K., Haramaty, L., and Falkowski, P. G.: The demise of the marine
783 cyanobacterium, *Trichodesmium* spp., via an autocatalyzed cell death pathway, Limnology
784 and Oceanography, 49, 997-1005, 2004.

785 Berman-Frank, I., Rosenberg, G., Levitan, O., Haramaty, L., and Mari, X.: Coupling between
786 autocatalytic cell death and transparent exopolymeric particle production in the marine
787 cyanobacterium *Trichodesmium*, Environmental Microbiology, 9, 1415-1422, 10.1111/j.1462-
788 2920.2007.01257.x, 2007.

789 Berthelot, H., Moutin, T., L'Helguen, S., Leblanc, K., Hélias, S., Grosso, O., Leblond, N.,
790 Charrière, B., and Bonnet, S.: Dinitrogen fixation and dissolved organic nitrogen fueled
791 primary production and particulate export during the VAHINE mesocosm experiment (New
792 Caledonia lagoon), Biogeosciences, 12, 4099-4112, 10.5194/bg-12-4099-2015, 2015.

793 Beversdorf, L., White, A., Björkman, K., Letelier, R., and Karl, D.: Phosphonate metabolism
794 by *Trichodesmium* IMS101 and the production of greenhouse gases, Limnology and
795 Oceanography, 55, 1768-1778, 2010.

796 Bidle, K. D., and Falkowski, P. G.: Cell death in planktonic, photosynthetic microorganisms,
797 Nature Reviews Microbiology, 2, 643-655, 2004.

Bidle, K. D.: The molecular ecophysiology of programmed cell death in marine phytoplankton, Annual Review Marine Science, 7, 341-375, 2015.

Bonnet, S., Berthelot, H., Turk-Kubo, K., Fawcett, S., Rahav, E., l'Helguen, S., and Berman-Frank, I.: Dynamics of N_2 fixation and fate of diazotroph-derived nitrogen in a low nutrient low chlorophyll ecosystem: results from the VAHINE mesocosm experiment (New Caledonia), Biogeosciences, 12, 19579-19626, doi:10.5194/bgd-12-19579-2015, 2015.

Bonnet, S., Moutin, T., Rodier, M., Grisoni, J. M., Louis, F., Folcher, E., Bourgeois, B., Boré, J. M., and Renaud, A.: Introduction to the project VAHINE: Variability of vertical and trophic transfer of diazotroph derived N in the South West Pacific, Biogeosciences, doi:10.5194/bg-2015-615, 2016a.

Bonnet, S., Berthelot, H., Turk-Kubo, K., Cornet-Barthaux, V., Fawcett, S., Berman-Frank, I., Barani, A., Dekeazemacker, J., Benavides, M., Charrière, B., and Capone, D.: *Trichodesmium* blooms support diatom growth in the Southwest Pacific Ocean, Limnology and Oceanography, 2016b. In Press.

Brown, J. M., LaBarre, B. A., and Hewson, I.: Characterization of *Trichodesmium*-associated viral communities in the eastern Gulf of Mexico, FEMS Microbiology Ecology, 84, 603-613, 2013.

Brussaard, C. P. D., Mari, X., Van Bleijswijk, J. D. L., and Veldhuis, M. J. W.: A mesocosm study of Phaeocystis globosa (Prymnesiophyceae) population dynamics - II. Significance for the microbial community, Harmful Algae, 4, 875-893, 2005.

Brussaard, C. R. D.: Optimization of procedures for counting viruses by flow cytometry, App. Environmental Microbiology, 70, 1506-1513, 2003.

Capone, D., Burns, J., Montoya, J., Michaels, A., Subramaniam, A., and Carpenter, E.: New nitrogen input to the tropical North Atlantic Ocean by nitrogen fixation by the cyanobacterium, *Trichodesmium* spp, Global Biogeochemical Cycles, 19, 2004.

Capone, D. G., and Carpenter, E. J.: Nitrogen fixation in the marine environment, Science, 217, 1140-1142, 1982.

Capone, D. G., Zehr, J. P., Paerl, H. W., Bergman, B., and Carpenter, E. J.: *Trichodesmium*, a globally significant marine cyanobacterium, Science, 276, 1221-1229, 1997.

Capone, D. G., Subramaniam, A., Montoya, J. P., Voss, M., Humborg, C., Johansen, A. M., Siefert, R. L., and Carpenter, E. J.: An extensive bloom of the N_2-fixing cyanobacterium *Trichodesmium erythraeum* in the central Arabian Sea, Marine Ecology Progress Series, 172, 281-292, 1998.

Castruita, M., Saito, M., Schottel, P., Elmegreen, L., Myneni, S., Stiefel, E., and Morel, F. M.: Overexpression and characterization of an iron storage and DNA-binding Dps protein from *Trichodesmium erythraeum*, Applied and Environmental Microbiology, 72, 2918-2924, 2006.

Chappell, P. D., and Webb, E. A.: A molecular assessment of the iron stress response in the two phylogenetic clades of *Trichodesmium*, Environmental Microbiology, 12, 13-27, 10.1111/j.1462-2920.2009.02026.x, 2010.

838 Coleman, M. L., and Chisholm, S. W.: Ecosystem-specific selection pressures revealed
839 through comparative population genomics, Proceedings of the National Academy of Sciences,
840 107, 18634-18639, 2010.

841 Dandonneau, Y., and Gohin, F.: Meridional and seasonal variations of the sea surface
842 chlorophyll concentration in the southwestern tropical Pacific (14 to 32 S, 160 to 175 E), Deep
843 Sea Research Part A. Oceanographic Research Papers, 31, 1377-1393, 1984.

844 Dowd, S. E., Callaway, T. R., Wolcott, R. D., Sun, Y., McKeehan, T., Hagevoort, R. G., and
845 Edrington, T. S.: Evaluation of the bacterial diversity in the feces of cattle using 16S rDNA
846 bacterial tag-encoded FLX amplicon pyrosequencing (bTEFAP), BMC microbiology, 8, 125,
847 2008.

848 Dupouy, C., Benielli-Gary, D., Neveux, J., Dandonneau, Y., and Westberry, T. K.: An
849 algorithm for detecting *Trichodesmium* surface blooms in the South Western Tropical Pacific,
850 Biogeosciences, 8, 3631-3647, 10.5194/bg-8-3631-2011, 2011.

851 Dyhrman, S. T., Chappell, P. D., Haley, S. T., Moffett, J. W., Orchard, E. D., Waterbury, J. B.,
852 and Webb, E. A.: Phosphonate utilization by the globally important marine diazotroph
853 *Trichodesmium*, Nature, 439, 68-71, 2006.

854 Edgar, R. C.: UPARSE: highly accurate OTU sequences from microbial amplicon reads,
855 Nature Methods, 10, 996-998, 2013.

856 Engel, A.: The role of transparent exopolymer particles (TEP) in the increase in apparent
857 particle stickiness (alpha) during the decline of a diatom bloom, Journal of Plankton Research,
858 22, 485-497, 2000.

859 Evans, C., Malin, G., Mills, G. P., and Wilson, W. H.: Viral infection of *Emiliania huxleyi*
860 (prymnesiophyceae) leads to elevated production of reactive oxygen species, Journal of
861 Phycology, 42, 1040-1047, 2006.

862 Frydenborg, B. R., Krediet, C. J., Teplitski, M., and Ritchie, K. B.: Temperature-dependent
863 inhibition of opportunistic vibrio pathogens by native coral commensal bacteria, Microbial
864 Ecology, 67, 392-401, 2014.

865 Georgiou, T., Yu, Y.-T., Ekunwe, S., Buttner, M., Zuurmond, A.-M., Kraal, B., Kleanthous,
866 C., and Snyder, L.: Specific peptide-activated proteolytic cleavage of *Escherichia co*li
867 elongation factor Tu, Proceedings of the National Academy of Sciences, 95, 2891-2895, 1998.

868 Guo, C., and Tester, P. A.: Toxic effect of the bloom-forming *Trichodesmium* sp.
869 (Cyanophyta) to the copepod Acartia tonsa, Natural Toxins, 2, 222-227, 1994.

870 Hamady, M., Walker, J. J., Harris, J. K., Gold, N. J., and Knight, R.: Error-correcting
871 barcoded primers for pyrosequencing hundreds of samples in multiplex, Nature Methods, 5,
872 235-237, 2008.

873 Havaux, M., Guedeney, G., Hagemann, M., Yeremenko, N., Matthijs, H. C., and Jeanjean, R.:
874 The chlorophyll-binding protein IsiA is inducible by high light and protects the
875 cyanobacterium *Synechocystis* PCC6803 from photooxidative stress, FEBS Letters, 579,
876 2289-2293, 2005.

Herbland, A., Le Bouteiller, A., and Raimbault, P.: Size structure of phytoplankton biomass in the equatorial Atlantic Ocean, Deep Sea Research Part A. Oceanographic Research Papers, 32, 819-836, 1985.

Hewson, I., Govil, S. R., Capone, D. G., Carpenter, E. J., and Fuhrman, J. A.: Evidence of *Trichodesmium* viral lysis and potential significance for biogeochemical cycling in the oligotrophic ocean, Aquatic Microbial Ecology, 36, 1-8, 2004.

Hewson, I., Poretsky, R. S., Dyhrman, S. T., Zielinski, B., White, A. E., Tripp, H. J., Montoya, J. P., and Zehr, J. P.: Microbial community gene expression within colonies of the diazotroph, *Trichodesmium*, from the Southwest Pacific Ocean, ISME Journal, 3, 1286-1300, 10.1038/ismej.2009.75, 2009.

Hmelo, L. R., Van Mooy, B. A. S., and Mincer, T. J.: Characterization of bacterial epibionts on the cyanobacterium *Trichodesmium*, Aquatic Microbial Ecology, 67, 1-U119, 10.3354/ame01571, 2012.

Holmes, R. M., Aminot, A., Kérouel, R., Hooker, B. A., and Peterson, B. J.: A simple and precise method for measuring ammonium in marine and freshwater ecosystems, Canadian Journal of Fisheries and Aquatic Sciences, 56, 1801-1808, 10.1139/f99-128, 1999.

Hove-Jensen, B., Zechel, D. L., and Jochimsen, B.: Utilization of Glyphosate as Phosphate Source: Biochemistry and Genetics of Bacterial Carbon-Phosphorus Lyase, Microbiology and Molecular Biology Reviews, 78, 176-197, 2014.

Hunt, B. P. V., Bonnet, S., Berthelot, H., Conroy, B. J., Foster, R., and Pagano, M.: Contribution and pathways of diazotroph derived nitrogen to zooplankton during the VAHINE mesocosm experiment in the oligotrophic New Caledonia lagoon, Biogeosciences Discussions, doi:10.5194/bg-2015-614, 2016.

Ivars-Martinez, E., Martin-Cuadrado, A.-B., D'Auria, G., Mira, A., Ferriera, S., Johnson, J., Friedman, R., and Rodriguez-Valera, F.: Comparative genomics of two ecotypes of the marine planktonic copiotroph *Alteromonas macleodii* suggests alternative lifestyles associated with different kinds of particulate organic matter, The ISME Journal, 2, 1194-1212, 2008.

Jacquet, S., Heldal, M., Iglesias-Rodriguez, D., Larsen, A., Wilson, W., and Bratbak, G.: Flow cytometric analysis of an *Emiliana huxleyi* bloom terminated by viral infection, Aquatic Microbial Ecology, 27, 111-124, 2002.

Jacquet, S., Delesalle, B., Torréton, J.-P., and Blanchot, J.: Response of phytoplankton communities to increased anthropogenic influences (southwestern lagoon, New Caledonia), Marine Ecology Progress Series, 320, 65-78, 2006.

Jeanjean, R., Zuther, E., Yeremenko, N., Havaux, M., Matthijs, H. C., and Hagemann, M.: A photosystem 1 *psaFJ*-null mutant of the cyanobacterium *Synechocystis* PCC 6803 expresses the *isiAB* operon under iron replete conditions, FEBS letters, 549, 52-56, 2003.

Kerbrat, A.-S., Darius, H. T., Pauillac, S., Chinain, M., and Laurent, D.: Detection of ciguatoxin-like and paralysing toxins in *Trichodesmium* spp. from New Caledonia lagoon, Marine Pollution Bulletin, 61, 360-366, 2010.

916 Kopylova, E., Noé, L., and Touzet, H.: SortMeRNA: fast and accurate filtering of ribosomal
917 RNAs in metatranscriptomic data, Bioinformatics, 28, 3211-3217, 2012.

918 Langmead, B., and Salzberg, S. L.: Fast gapped-read alignment with Bowtie 2, Nature
919 Methods, 9, 357-359, 2012.

920 Latifi, A., Jeanjean, R., Lemeille, S., Havaux, M., and Zhang, C.-C.: Iron starvation leads to
921 oxidative stress in *Anabaena* sp. strain PCC 7120, Journal of Bacteriology, 187, 6596-6598,
922 2005.

923 Laudenbach, D. E., and Straus, N. A.: Characterization of a cyanobacterial iron stress-induced
924 gene similar to psbC, Journal of Bacteriology, 170, 5018-5026, 1988.

925 Leblanc, K., Cornet, V., Caffin, M., Rodier, M., Desnues, A., Berthelot, H., Turk-Kubo, K.,
926 and Heliou, J.: Phytoplankton community structure in the VAHINE mesocosm experiment,
927 Biogeosciences Discussions., doi:10.5194/bg-2015-605, 2016.

928 Lehahn, Y., Koren, I., Schatz, D., Frada, M., Sheyn, U., Boss, E., Efrati, S., Rudich, Y.,
929 Trainic, M., and Sharoni, S.: Decoupling physical from biological processes to assess the
930 impact of viruses on a mesoscale algal bloom, Current Biology, 24, 2041-2046, 2014.

931 Luo, Y.-W., Doney, S., Anderson, L., Benavides, M., Berman-Frank, I., Bode, A., Bonnet, S.,
932 Boström, K., Böttjer, D., and Capone, D.: Database of diazotrophs in global ocean:
933 abundance, biomass and nitrogen fixation rates, Earth System Science Data, 4, 47-73, 2012.

934 Mackey, K. R., Post, A. F., McIlvin, M. R., Cutter, G. A., John, S. G., and Saito, M. A.:
935 Divergent responses of Atlantic coastal and oceanic *Synechococcus* to iron limitation,
936 Proceedings of the National Academy of Sciences, 112, 9944-9949, 2015.

937 Martin, M.: Cutadapt removes adapter sequences from high-throughput sequencing reads,
938 EMBnet. Journal, 17, pp. 10-12, 2011.

939 Martinez, A., Tyson, G. W., and DeLong, E. F.: Widespread known and novel phosphonate
940 utilization pathways in marine bacteria revealed by functional screening and metagenomic
941 analyses, Environmental Microbiology, 12, 222-238, 10.1111/j.1462-2920.2009.02062.x,
942 2010.

943 Martínez, A., Osburne, M. S., Sharma, A. K., DeLong, E. F., and Chisholm, S. W.: Phosphite
944 utilization by the marine picocyanobacterium *Prochlorococcus* MIT9301, Environmental
945 Microbiology, 14, 1363-1377, 2012.

946 Massana, R., Murray, A. E., Preston, C. M., and DeLong, E. F.: Vertical distribution and
947 phylogenetic characterization of marine planktonic Archaea in the Santa Barbara Channel,
948 Applied and Environmental Microbiology, 63, 50-56, 1997.

949 Michel, K. P., and Pistorius, E. K.: Adaptation of the photosynthetic electron transport chain
950 in cyanobacteria to iron deficiency: the function of IdiA and IsiA, Physiologia Plantarum, 120,
951 36-50, 2004.

952 Mohr, W., Grosskopf, T., Wallace, D. W., and LaRoche, J.: Methodological underestimation
953 of oceanic nitrogen fixation rates, PLOS One, 5, e12583, 2010.

954 Montoya, J. P., Voss, M., Kahler, P., and Capone, D. G.: A simple, high-precision, high-
955 sensitivity tracer assay for N_2 fixation, Applied and Environmental Microbiology, 62, 986-
956 993, 1996.

957 Mulholland, M. R.: The fate of nitrogen fixed by diazotrophs in the ocean, Biogeosciences, 4,
958 37-51, 2007.

959 O'Neil, J. M., and Roman, M. R.: Ingestion of the Cyanobacterium *Trichodesmium* spp by
960 Pelagic Harpacticoid Copepods *Macrosetella*, *Miracia* and *Oculostella*, Hydrobiologia, 293,
961 235-240, 1994.

962 O'Neil, J. M.: The colonial cyanobacterium *Trichodesmium* as a physical and nutritional
963 substrate for the harpacticoid copepod *Macrosetella gracilis*, Journal of Plankton Research,
964 20, 43-59, 1998.

965 Ohki, K.: A possible role of temperate phage in the regulation of *Trichodesmium* biomass,
966 Bulletin de l'institute oceanographique, Monaco, 19, 287-291, 1999.

967 Orchard, E., Webb, E., and Dyhrman, S.: Characterization of phosphorus-regulated genes in
968 *Trichodesmium* spp., The Biological Bulletin, 205, 230-231, 2003.

969 Paerl, H. W., Priscu, J. C., and Brawner, D. L.: Immunochemical localization of nitrogenase in
970 marine *Trichodesmium* aggregates: Relationship to N_2 fixation potential, Applied and
971 Environmental Microbiology, 55, 2965-2975, 1989.

972 Passow, U., and Alldredge, A. L.: A dye binding assay for the spectrophotometeric
973 measurement of transparent exopolymer particles (TEP), Limnology and Oceanography, 40,
974 1326-1335, 1995.

975 Pfreundt, U., Kopf, M., Belkin, N., Berman-Frank, I., and Hess, W. R.: The primary
976 transcriptome of the marine diazotroph *Trichodesmium erythraeum* IMS101, Scientific
977 Reports, 4, 2014.

978 Pfreundt, U., Van Wambeke, F., Caffin, M., Bonnet, S., and Hess, W. R.: Succession within
979 the prokaryotic communities during the VAHINE mesocosms experiment in the New
980 Caledonia lagoon, Biogeosciences, 13, 2319-2337, doi:10.5194/bg-13-2319-2016, 2016.

981 Pichon, D., Cudennec, B., Huchette, S., Djediat, C., Renault, T., Paillard, C., and Auzoux-
982 Bordenave, S.: Characterization of abalone *Haliotis tuberculata–Vibrio harveyi* interactions in
983 gill primary cultures, Cytotechnology, 65, 759-772, 2013.

984 Pinto, F. L., Thapper, A., Sontheim, W., and Lindblad, P.: Analysis of current and alternative
985 phenol based RNA extraction methodologies for cyanobacteria, BMC Molecular Biology, 10,
986 1, 2009.

987 Polyviou, D., Hitchcock, A., Baylay, A. J., Moore, C. M., and Bibby, T. S.: Phosphite
988 utilization by the globally important marine diazotroph *Trichodesmium*, Environmental
989 Microbiology Reports, 7, 824-830, 2015.

990 Pujo-Pay, M., and Raimbault, P.: Improvement of the wet-oxidation procedure for
991 simultaneous determination of particulate organic nitrogen and phosphorus collected on filters,
992 Marine Ecology-Progress Series, 105, 203–207, 10.3354/meps105203, 1994.

Quast, C., Pruesse, E., Yilmaz, P., Gerken, J., Schweer, T., Yarza, P., Peplies, J., and Glöckner, F. O.: The SILVA ribosomal RNA gene database project: improved data processing and web-based tools, Nucleic Acids Research, 41, D590-D596, 10.1093/nar/gks1219, 2013.

Rahav, E., Herut, B., Levi, A., Mulholland, M., and Berman-Frank, I.: Springtime contribution of dinitrogen fixation to primary production across the Mediterranean Sea, Ocean Science, 9, 489-498, 2013.

Rodier, M., and Le Borgne, R.: Population dynamics and environmental conditions affecting *Trichodesmium* spp. (filamentous cyanobacteria) blooms in the south-west lagoon of New Caledonia, Journal of Experimental Marine Biology and Ecology, 358, 20-32, 10.1016/j.jembe.2008.01.016, 2008.

Rodier, M., and Le Borgne, R.: Population and trophic dynamics of *Trichodesmium thiebautii* in the SE lagoon of New Caledonia. Comparison with *T. erythraeum* in the SW lagoon, Marine Pollution Bulletin, 61, 349-359, 2010.

Shaked, Y.: Iron redox dynamics and biogeochemical cycling in the epilimnion of Lake Kinneret, PhD thesis, Hebrew University of Jerusalem, 2002.

Sheridan, C. C., Steinberg, D. K., and Kling, G. W.: The microbial and metazoan community associated with colonies of *Trichodesmium* spp.: a quantitative survey, Journal of Plankton Research, 24, 913-922, 2002.

Siddiqui, P. J., Bergman, B., Bjorkman, P. O., and Carpenter, E. J.: Ultrastructural and chemical assessment of poly-beta-hydroxybutyric acid in the marine cyanobacterium *Trichodesmium thiebautii*, FEMS Microbiology Letters, 73, 143-148, 1992.

Smetacek, V.: Role of sinking in diatom life-history cycles: ecological, evolutionary and geological significance, Marine Biology, 84, 239-251, 1985.

Snow, J. T., Polyviou, D., Skipp, P., Chrismas, N. A., Hitchcock, A., Geider, R., Moore, C. M., and Bibby, T. S.: Quantifying Integrated Proteomic Responses to Iron Stress in the Globally Important Marine Diazotroph *Trichodesmium*, PLOS One, 10, e0142626, 2015.

Spungin, D., Berman-Frank, I., and Levitan, O.: *Trichodesmium's* strategies to alleviate phosphorus limitation in the future acidified oceans, Environmental Microbiology, 16, 1935-1947, 2014.

Spungin, D., Rosenberg, G., Bidle, K. D., and Berman-Frank, I.: Metacaspases and bloom demise in the marine cyanobacterium *Trichodesmium*, In Prep.

Strickland, J. D. H., and Parsons, T. R.: A Practical Handbook of Seawater Analysis, Fisheries Research Board of Canada, Ottawa, 1972.

Tandeau de Marsac, N., and Houmard, J.: Complementary chromatic adaptation: Physiological conditions and action spectra, in: Methods in Enzymology, Academic Press, 318-328, 1988.

Tarutani, K., Nagasaki, K., and Yamaguchi, M.: Viral impacts on total abundance and clonal composition of the harmful bloom-forming phytoplankton heterosigma akashiwo, Applied and Environmental Microbiology, 66, 4916-4920, 2000.

Thamatrakoln, K., Korenovska, O., Niheu, A. K., and Bidle, K. D.: Whole-genome expression analysis reveals a role for death-related genes in stress acclimation of the diatom *Thalassiosira pseudonana*, Environmental Microbiology, 14, 67-81, 2012.

Turk-Kubo, K., Frank, I., Hogan, M., Desnues, A., Bonnet, S., and Zehr, J.: Diazotroph community succession during the VAHINE mesocosms experiment (New Caledonia Lagoon), Biogeosciences 12, 7435-7452, doi:10.5194/bg-12-7435-2015, 2015.

Van Mooy, B. A., Hmelo, L. R., Sofen, L. E., Campagna, S. R., May, A. L., Dyhrman, S. T., Heithoff, A., Webb, E. A., Momper, L., and Mincer, T. J.: Quorum sensing control of phosphorus acquisition in *Trichodesmium* consortia, The ISME Journal, 6, 422-429, 2012.

Van Wambeke, F., Pfreundt, U., Barani, A., Berthelot, H., Moutin, T., Rodier, M., Hess, W. R., and Bonnet, S.: Heterotrophic bacterial production and metabolic balance during the VAHINE mesocosm experiment in the New Caledonia lagoon, Biogeosciences Discussions, 12, 19861-19900, doi:10.5194/bgd-12-19861-2015, 2015.

Vardi, A., Berman-Frank, I., Rozenberg, T., Hadas, O., Kaplan, A., and Levine, A.: Programmed cell death of the dinoflagellate *Peridinium gatunense* is mediated by CO_2 limitation and oxidative stress, Current Biology: CB, 9, 1061-1064, 1999.

Vardi, A., Haramaty, L., Van Mooy, B. A., Fredricks, H. F., Kimmance, S. A., Larsen, A., and Bidle, K. D.: Host–virus dynamics and subcellular controls of cell fate in a natural coccolithophore population, Proceedings of the National Academy of Sciences, 109, 19327-19332, 2012.

Walsby, A. F.: The properties and bouyancy providing role of gas vacuoles in *Trichodesmium*, British Phycological Journal, 13, 103-116, 1978.

Weitz, J. S., and Wilhelm, S. W.: Ocean viruses and their effects on microbial communities and biogeochemical cycles, F1000 Biology Reports, 4, 17, 2012.

Wu, Z., Jenkins, B. D., Rynearson, T. A., Dyhrman, S. T., Saito, M. A., Mercier, M., and Whitney, L. P.: Empirical bayes analysis of sequencing-based transcriptional profiling without replicates, BMC Bioinformatics, 11, 564, 2010.

Zehr, J. P.: Nitrogen fixation in the Sea: Why Only *Trichodesmium*, in: Molecular Ecology of Aquatic Microbes, edited by: Joint, I., NATO ASI Series, Springer-Verlag, Heidelberg, 335-363, 1995.

Figure legends

Figure 1. Temporal dynamics of pre-bloom measurements in the lagoon waters (a) Chl *a* concentrations (µg L^{-1}), (b) Virus like particles (VLP, mL^{-1} x 10^6), (c) N_2 fixation rates (nmol L^{-1} h^{-1}) and particulate organic nitrogen (PON, µmol L^{-1}). (d) Changes in the concentrations of

transparent exopolymeric particles (TEP, µg GX L^{-1}) and particulate organic carbon (POC, µmol L^{-1}). Water was sampled from in the lagoon outside the VAHINE mesocosms, at 1 m depth (surface) throughout the experimental period from day 2 to 23 (n=3). For VLP, the standard error for technical replicates (n=3) was < 1 %, which is smaller than symbol size.

Figure 2. (a-c) Dense surface blooms of *Trichodesmium* observed outside the mesocosms in the lagoon waters on day 23 at 12:00. Photos illustrate the spatial heterogeneity of the surface accumulations and the high density of the biomass. (d-e) To examine the mechanistic of demise (Experiment 1), *Trichodesmium* filaments and colonies were collected by plankton net (mesh size, 80 µm) from the dense surface bloom (day 23, 12:00 h; designated T_0) and resuspended in 0.2 µm pore-size filtered seawater (FSW) in six 4.5 L bottles. Bottles were incubated on-deck in running-seawater pools with ambient surface temperature (~ 26 °C) at 50 % of the surface irradiance. Bottles were sampled every 2-4 h for different parameters until the biomass crashed. (f) Temporal changes in Chl *a* concentrations in the bottles from the time of biomass collection and resuspension in the bottles until the *Trichodesmium* biomass crashed ~ 24 h after the experiment began (n=3-6). Photo c. courtesy of A. Renaud.

Figure 3. Dynamics of microbial community abundance and diversity during *Trichodesmium* surface bloom as obtained by 16S rRNA gene sequencing for samples collected from the surface waters outside the mesocosms during *Trichodesmium* surface accumulation (bloom) (short-term experiment 1). Pie charts show the changes in dominant groups during the *Trichodesmium* bloom and crash from two replicate incubation bottles (please note, *Oscillatoriales* consisted only of *Trichodesmium* in this experiment). The graphs below show the respective temporal dynamics of *Trichodesmium* (gray circles) and *Alteromonas* (white triangles), the dominant bacterial species during the incubation expreriment.

Figure 4. Short-term experiment 2 - measurements from the lagoon waters following *Trichodemsium* bloom on day 23. (a) Virus like particles (VLP, mL^{-1} x 10^6) and *Trichodesmium* abundance (trichomes L^{-1}) derived from qPCR-based abundances of *Trichodesmium nifH* gene copies (Bonnet et al. 2016b) based on the assumption of 100 gene-copies per trichome (b) N_2 fixation rates (nmol L^{-1} h^{-1}), particulate organic nitrogen (PON, µmol L^{-1}) and ammonium concentrations (NH_4^+, µmol L^{-1}). (c) Changes in the concentrations of transparent exopolymeric particles (TEP, µg GX L^{-1}) and particulate organic carbon (POC, µmol L^{-1}). For experiment 2, seawater from the surface bloom was collected 5 h after the initial surface bloom was sighted (day 23, 17:00) by directly filling 20 L polyethylene carboys

gently to avoid destroying biomass. Bottles were placed in on-deck incubators filled with running seawater to maintain ambient surface temperature (~ 26 °C) and covered with neutral screening at 50 % surface irradiance levels. For all parameters, replicates were n=3. For VLP, the standard error for technical replicates (n=3) was < 1 %, which is smaller than symbol size.

Figure 5. (a) Expression of alkaline phosphatase associated genes *phoA* and *phoX* (Tery_3467 and Tery_3845), phosphite utilization genes *ptxA*, *ptxB* and *ptxC* (Tery_0365- Tery_0367), and phosphonate utilization genes (*phn* genes, Tery_4993, Tery_4994, Tery_4995, Tery_4996*, Tery_4997, Tery_4998, Tery_4999, Tery_5000, Tery_5001 Tery_5002 and Tery_5003). Asterisks near locus tag numbers indicate gene duplicates. (b) Iron-related genes, *isiB* (Tery_1666), *isiA* (Tery_1667), *idiA* (Tery_3377), and ferritin DPS gene *dpsA* (Tery_4282). Bars represent log2 fold changes of corresponding genes at T_8 (8 hours after T_0) and T_{22} (22 hours after T_0) in comparison to T_0. Significant expression was tested with ASC (Wu et al., 2010) and marked with an asterisk. Black asterisks represent significant change from T_0. A gene was called differentially expressed if $P > 0.98$ (posterior probability).

Figure 6. (a) Dynamics of caspase-specific activity rates (pmol L^{-1} min^{-1}) of *Trichodesmium* in the New Caledonian lagoon during bloom accumulation and bloom demise, sampled during experiment 1. Samples (n=6) collected from the bloom (day 23, 12:00 T_0), were incubated on-deck in an incubator fitted with running seawater to maintain ambient surface temperature (~ 26 °C). (b) Transcript accumulation of metacaspase genes in the *Trichodesmium* bloom during the short-term incubation experiment. Metacaspase genes are *TeMC1* (Tery_2077), *TeMC2* (Tery_2689), *TeMC3* (Tery_3869), *TeMC4* (Tery_2471), *TeMC5* (Tery_2760), *TeMC6* (Tery_2058), *TeMC7* (Tery_1841), *TeMC8* (Tery_0382), *TeMC9* (Tery_4625), *TeMC10* (Tery_2624), *TeMC11* (Tery_2158) and *TeMC12* (Tery_2963). Bars represent log2 fold changes at T_8 (8 hours after T_0) and T_{22} (22 hours since T_0) in comparison to T_0. Significant expression was tested with ASC (Wu et al., 2010) and marked with an asterisk. Black asterisks represent significant change from T_0. A gene was called differentially expressed if $P > 0.98$ (posterior probability).

Figure 7. Change in gas vesicle protein (*gvp*) genes as obtained from metatranscriptomic analyses of the *Trichodesmium* bloom from peak to collapse (experiment 1). *gvpA* genes (Tery_2330 and Tery_2335*) encode the main constituent of the gas vesicles that forms the essential core of the structure; *gvpN* (Tery_2329 and Tery_2334) *gvpK* (Tery_2322), *gvpG* (Tery_2338) and *gvpL/gvpF* (Tery_2339 and Tery_2340*) encode vesicle synthesis proteins.

Bars represent log2 fold changes at T_8 (8 hours after T_0) and T_{22} (22 hours since T_0) in comparison to T_0. Significant expression was tested with ASC (Wu et al., 2010) and marked with an asterisk. Black asterisks represent significant change from T_0. A gene was called differentially expressed if $P > 0.98$ (posterior probability).

Figure 1

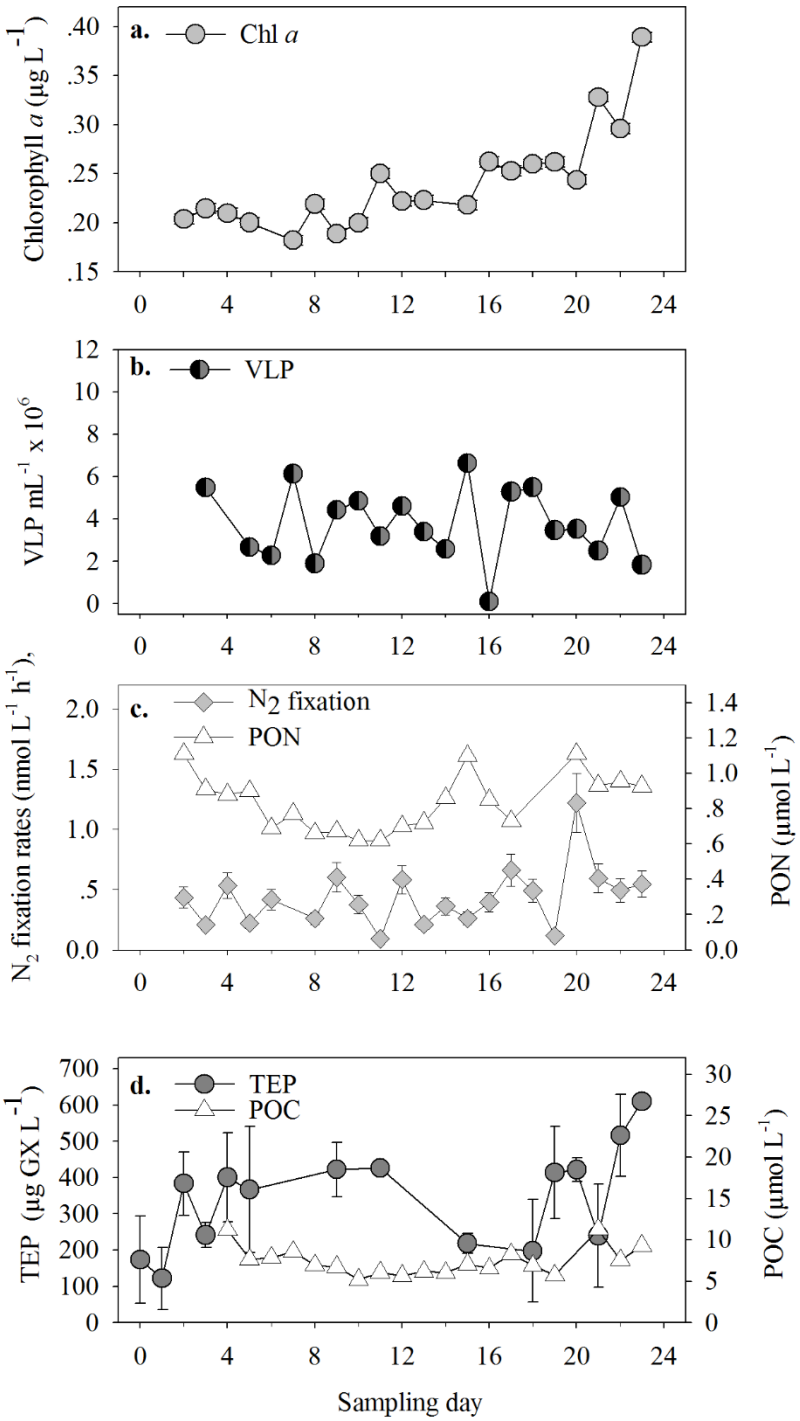
a.
Chl a
Chlorophyll a (µg L-1)
b.
VLP
VLP mL-1 x 10^6
c.
N2 fixation
PON
N2 fixation rates (nmol L-1 h-1),
PON (µmol L-1)
d.
TEP
POC
TEP (µg GX L-1)
POC (µmol L-1)
Sampling day

Figure 2

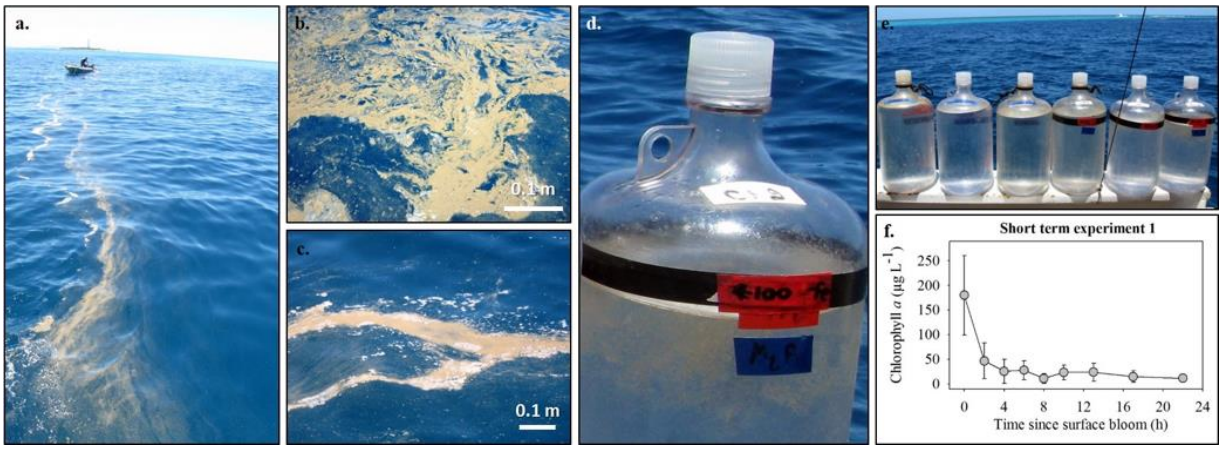
a.
b.
0.1 m
c.
0.1 m
d.
e.
f.
Short term experiment 1
Chlorophyll a (µg L-1)
250
200
150
100
50
0
0
4
8
12
16
20
24
Time since surface bloom (h)

Figure 3

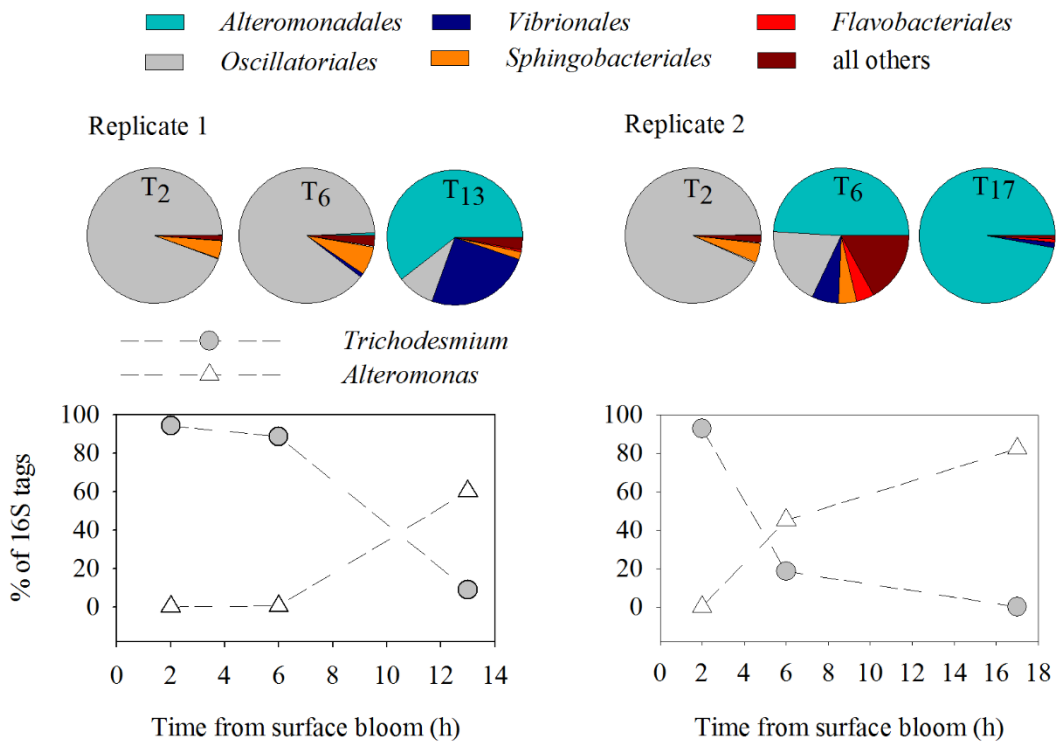
Alteromonadales
Oscillatoriales
Vibrionales
Sphingobacteriales
Flavobacteriales
all others
Replicate 1
T2
T6
T13
Replicate 2
T2
T6
T17
Trichodesmium
Alteromonas
% of 16S tags
100
80
60
40
20
0
0 2 4 6 8 10 12 14
Time from surface bloom (h)
100
80
60
40
20
0
0 2 4 6 8 10 12 14 16 18
Time from surface bloom (h)

Figure 4

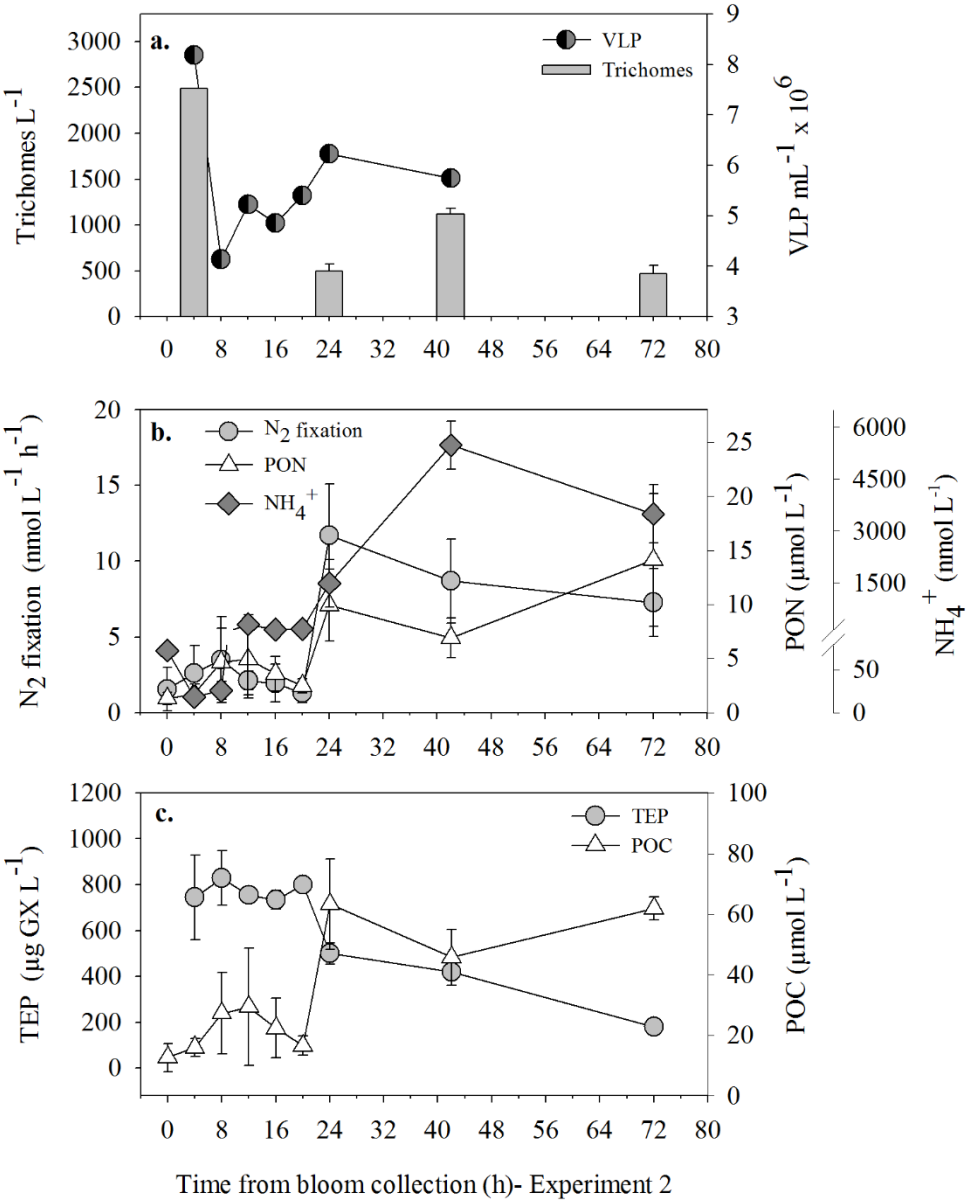
a.
VLP
Trichomes
Trichomes L-1
VLP mL-1 x 10^6
b.
N2 fixation
PON
NH4+
N2 fixation (nmol L-1 h-1)
PON (µmol L-1)
NH4+ (nmol L-1)
c.
TEP
POC
TEP (µg GX L-1)
POC (µmol L-1)
Time from bloom collection (h)- Experiment 2

Figure 5

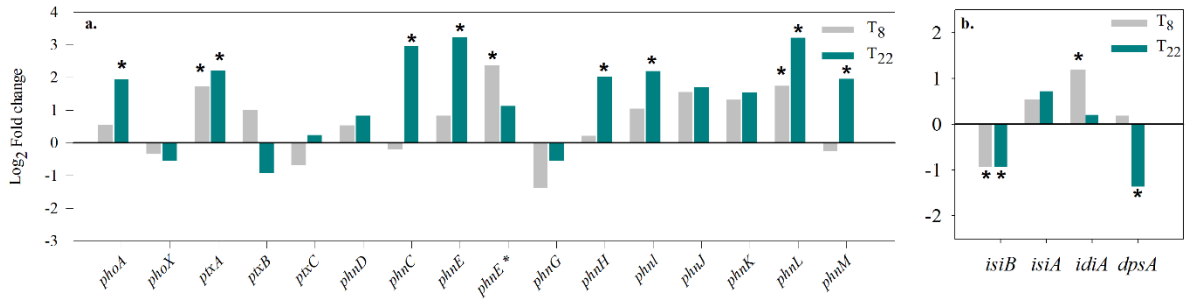
a.
b.
T8
T22
Log2 Fold change
phoA
phoX
ptxA
ptxB
ptxC
phnD
phnC
phnE
phnE*
phnG
phnH
phnI
phnJ
phnK
phnL
phnM
isiB
isiA
idiA
dpsA

Figure 6

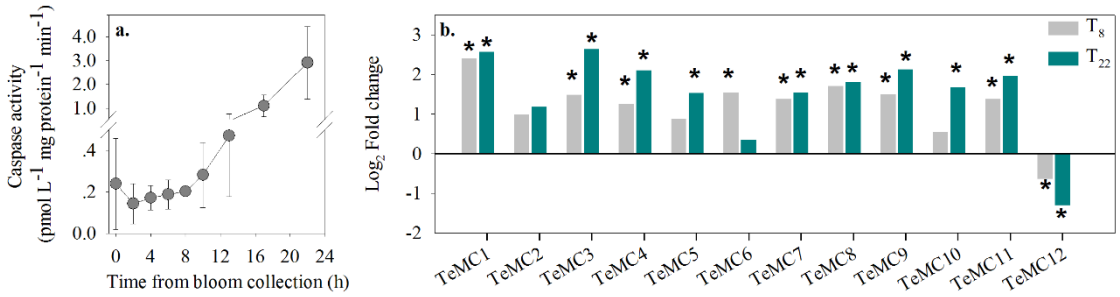
a.
Caspase activity
(pmol L-1 mg protein-1 min-1)
4.0
3.0
2.0
1.0
.4
.2
0.0
0
4
8
12
16
20
24
Time from bloom collection (h)
b.
Log2 Fold change
T8
T22
3
2
1
0
-1
-2
TeMC1
TeMC2
TeMC3
TeMC4
TeMC5
TeMC6
TeMC7
TeMC8
TeMC9
TeMC10
TeMC11
TeMC12

Figure 7

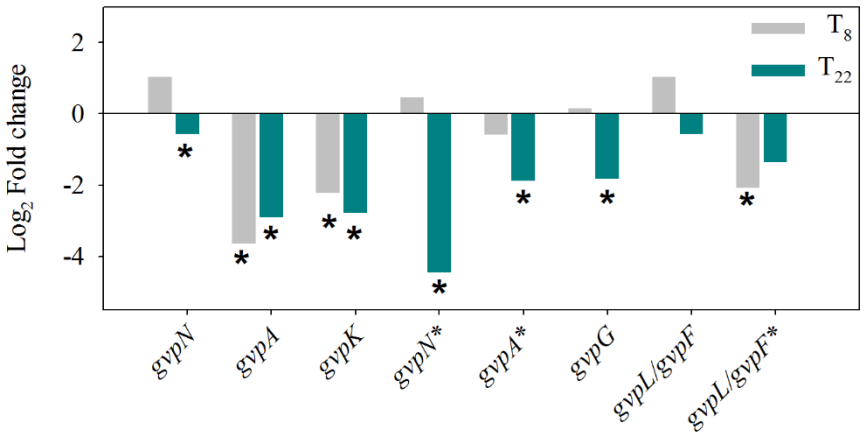
T8
T22
Log2 Fold change
2
0
-2
-4
gvpN
gvpA
gvpK
gvpN*
gvpA*
gvpG
gvpL/gvpF
gvpL/gvpF*

Supplementary information

Figure S1: Time line of sampling during pre-bloom days (yellow circles, days 1-23), and during experiment 1 (blue circles, days 23-24) and experiment 2 (green circles, days 23-26). For experiment 1, *Trichodesmium* filaments and colonies were collected from the dense surface bloom using a plankton net (mesh size, 80 µm) from surface water (day 23, 12:00 h; designated T_0). *Trichodesmium* was resuspended in filtered seawater (FSW) that was split to six 4.5 L bottles that were incubate (see below) and sampled every 2-4 h until the biomass crashed. For experiment 2, seawater from the surface bloom was collected 5 h after the initial surface bloom was sighted (day 23, 17:00) by directly filling 20 L polyethylene carboys using a Teflon® PFA pump. Carboys were sampled every 4 h during the first 23 hours and then after 42 h and 72 h since the beginning of the experiment. Bottles and carboys from both experiments were placed in on-deck incubators filled with running seawater to maintain ambient surface temperature (~ 26 °C) and covered with neutral screening at 50 % surface irradiance levels.

Figure S1

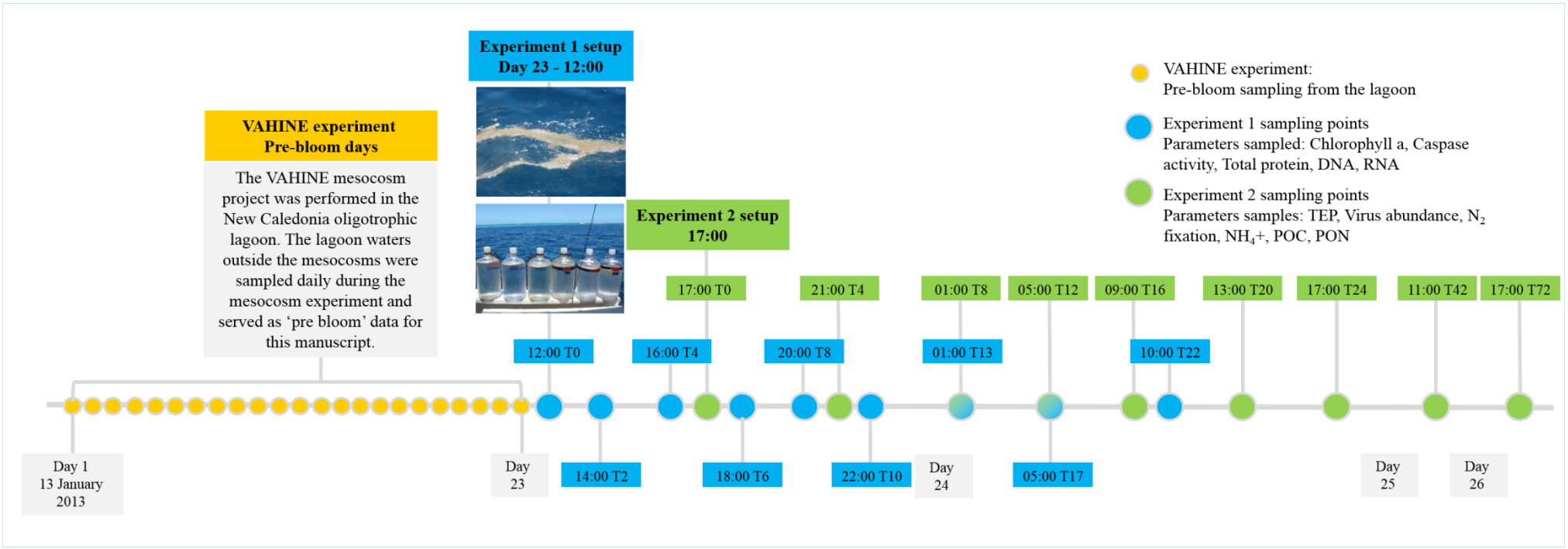
Experiment 1 setup
Day 23 - 12:00
VAHINE experiment
Pre-bloom days
The VAHINE mesocosm project was performed in the New Caledonia oligotrophic lagoon. The lagoon waters outside the mesocosms were sampled daily during the mesocosm experiment and served as 'pre bloom' data for this manuscript.
Experiment 2 setup
17:00
VAHINE experiment:
Pre-bloom sampling from the lagoon
Experiment 1 sampling points
Parameters sampled: Chlorophyll a, Caspase activity, Total protein, DNA, RNA
Experiment 2 sampling points
Parameters samples: TEP, Virus abundance, N_2 fixation, NH_4+, POC, PON
17:00 T0
21:00 T4
01:00 T8
05:00 T12
09:00 T16
13:00 T20
17:00 T24
11:00 T42
17:00 T72
12:00 T0
16:00 T4
20:00 T8
01:00 T13
10:00 T22
Day 1
13 January
2013
Day
23
14:00 T2
18:00 T6
22:00 T10
Day
24
05:00 T17
Day
25
Day
26

Table S1. Metatransciptomic changes of selected marker genes in samples from *Trichodesmium* bloom and crash. Metatranscriptomic samples were obtained from the *Trichodesmium* bloom on day 23 at three successive time points [(T_0, T_8 and T_{22}, representing 0, 8, and 22 h from surface bloom]. Table data provides the respective locus_tag in the *T. erythraeum* genome, gene name and annotation, expected fold-change calculated from the results of ASC (see methods section), log2 fold change, posterior probabilities for these fold-changes as calculated by ASC (significant if $P > 0.98$, in bold), and the reads per million reads (RPM) for each time point.

	Locus_tag	Symbol	Annotation	Fold-change (from ASC)			log2(Fold-change)			Posterior probabilities (P) from ASC						Reads per Million reads		
				(T8/T0)	(T22/T8)	(T22/T0)	(T8/T0)	(T22/T8)	(T22/T0)	P(T0/T8>2)	P(T8/T0>2)	P(T8/T22>2)	P(T22/T8>2)	P(T22/T0>2)	P(T0/T22>2)	T0	T8	T22
Gas Vesicle Protein (Gvp) formation	Tery_2322	gvpA	Gas vesicle synthesis protein- GvpA	0.53	NA	0.27	-0.92	NA	-1.88	0.43	0.00	NA	NA	0.00	0.81	8	0	0
	Tery_2323	gvpA	Gas vesicle synthesis protein- GvpA	0.41	NA	0.20	-1.29	NA	-2.32	0.73	0.00	NA	NA	0.00	0.93	15	0	0
	Tery_2324	gvpA	Gas vesicle synthesis protein- GvpA	0.12	4.09	0.48	-3.07	2.03	-1.06	**1.00**	0.00	0.00	**1.00**	0.00	0.97	5042	603	3009
	Tery_2325	gvpA	Gas vesicle synthesis protein- GvpA	0.12	2.12	0.26	-3.01	1.08	-1.94	**1.00**	0.00	0.00	0.79	0.00	**1.00**	4022	497	1285
	Tery_2329	gvpN	Gas vesicle protein- GvpN	0.58	0.45	0.26	-0.78	-1.14	-1.93	0.00	0.00	0.91	0.00	0.00	**1.00**	1964	1198	653
	Tery_2330	gvpA	Gas vesicle synthesis protein- GvpA	0.08	2.54	0.13	-3.65	1.35	-2.90	**1.00**	0.00	0.00	0.78	0.00	**1.00**	444	19	71
	Tery_2332	gvpK	Gas vesicle protein- GvpK	0.21	0.70	0.15	-2.22	-0.52	-2.78	**1.00**	0.00	0.01	0.00	0.00	**1.00**	1408	306	257
	Tery_2334	gvpN	Gas vesicle protein- GvpN	1.37	0.04	0.05	0.46	-4.57	-4.45	0.00	0.00	**1.00**	0.00	0.00	**1.00**	464	674	19
	Tery_2335	gvpA	Gas vesicle synthesis protein- GvpA	0.67	0.41	0.27	-0.58	-1.27	-1.88	0.00	0.00	0.90	0.00	0.00	**1.00**	479	335	164
	Tery_2338	gvpG	Gas vesicle protein- GvpG	1.11	0.26	0.28	0.15	-1.95	-1.84	0.00	0.00	**1.00**	0.00	0.00	**1.00**	431	505	152
	Tery_2339	gvpL/gvpF	Gas vesicle synthesis protein- GvpLGvpF	2.05	0.33	0.67	1.04	-1.61	-0.58	0.00	0.85	**1.00**	0.00	0.00	0.00	1608	3473	1371
	Tery_2340	gvpL/gvpF	Gas vesicle synthesis protein- GvpLGvpF	0.24	2.17	0.39	-2.08	1.12	-1.36	**1.00**	0.00	0.00	0.59	0.00	0.85	102	15	50
Phosphite Utalization genes	Tery_0365	ptxA	Phosphonate transport	3.29	1.18	4.59	1.72	0.24	2.20	0.00	**1.00**	0.00	0.01	**1.00**	0.00	16	72	105
	Tery_0366	ptxB	Phosphonate transport	1.99	0.27	0.53	0.99	-1.88	-0.92	0.00	0.48	**1.00**	0.00	0.00	0.36	193	412	130
	Tery_0367	ptxC	Phosphonate transport	0.62	1.93	1.18	-0.69	0.95	0.24	0.06	0.00	0.00	0.42	0.00	0.00	126	79	192
Phosphonate transporters and metabolism	Tery_4993	phnD	Phosphonate transport	1.44	1.19	1.77	0.53	0.25	0.82	0.00	0.01	0.00	0.00	0.23	0.00	61	97	142
	Tery_4994	phnC	Phosphonate transport	0.87	7.90	7.71	-0.20	2.98	2.95	0.00	0.00	0.00	**1.00**	**1.00**	0.00	34	30	344
	Tery_4995	phnE	Phosphonate transport	1.78	4.49	9.34	0.83	2.17	3.22	0.00	0.26	0.00	**1.00**	**1.00**	0.00	25	54	319
	Tery_4996	phnE	Phosphonate transport	5.18	0.40	2.19	2.37	-1.31	1.13	0.00	**1.00**	0.85	0.00	0.67	0.00	26	166	77
	Tery_4997	phnG	Membrane associated C-P lyase	0.39	2.97	0.68	-1.37	1.57	-0.55	0.79	0.00	0.00	0.75	0.00	0.22	17	0	15
	Tery_4998	phnH	Phosphonate metabolism	1.16	2.70	4.04	0.21	1.43	2.01	0.00	0.03	0.00	0.82	**0.99**	0.00	10	14	59
	Tery_4999	phnI	Phosphonate metabolism	2.06	1.77	4.58	1.05	0.82	2.20	0.00	0.56	0.00	0.33	**1.00**	0.00	12	35	80
	Tery_5000	phnJ	Membrane associated C-P lyase	2.93	0.91	3.24	1.55	-0.13	1.70	0.00	0.96	0.02	0.00	0.95	0.00	11	47	53
	Tery_5001	phnK	C-P lyase system	2.50	0.97	2.92	1.32	-0.05	1.54	0.00	0.83	0.02	0.01	0.89	0.00	11	39	46
	Tery_5002	phnL	C-P lyase system	3.36	2.09	9.25	1.75	1.06	3.21	0.00	**0.99**	0.00	0.58	**1.00**	0.00	11	55	149
	Tery_5003	phnM	Membrane associated C-P lyase	0.84	3.94	3.87	-0.25	1.98	1.95	0.04	0.00	0.00	**0.98**	**0.99**	0.00	13	11	74
Inorganic P transporters	Tery_3534	sphX	Phosphate bindig protein (regulated by P supply)	2.57	0.57	1.47	1.36	-0.82	0.55	0.00	**0.99**	0.22	0.00	0.02	0.00	71	202	136
	Tery_3537	pstS	Phosphate bindig protein	0.39	4.97	1.77	-1.34	2.31	0.83	0.87	0.00	0.00	**1.00**	0.23	0.00	62	19	146
	Tery_3539	pstS	Phosphate transport system permease protein 2	0.68	1.01	0.66	-0.56	0.01	-0.61	0.04	0.00	0.01	0.00	0.00	0.12	69	47	59
	Tery_3540	pstB	Inorganic P transporter	0.57	0.69	0.38	-0.80	-0.54	-1.40	0.12	0.00	0.08	0.00	0.00	0.92	162	94	77
	Tery_3583	pstC	Inorganic P transporter	2.17	1.34	3.25	1.12	0.42	1.70	0.00	0.68	0.00	0.03	**0.99**	0.00	25	66	111
Degradation of organic P sources	Tery_3467	phoA	Alkaline phosphatase	1.47	2.58	3.86	0.55	1.37	1.95	0.00	0.00	0.00	**1.00**	**1.00**	0.00	179	279	885
	Tery_3845	phoX	Alkaline phosphatase	0.79	0.87	0.68	-0.34	-0.20	-0.55	0.00	0.00	0.00	0.00	0.00	0.01	223	184	195
***Trichodesmium* Fe acquisition, storage, regulation ans quota reduction genes. (Gene list from Chappell and Webb 2009)**	Tery_1560	tonB	TonB family protein	2.38	0.37	0.88	1.25	-1.44	-0.19	0.00	**1.00**	**1.00**	0.00	0.00	0.00	979	2459	1096
	Tery_1666	fldA	Flavodoxin FldA	0.39	1.02	0.40	-1.34	0.02	-1.33	**1.00**	0.00	0.00	0.00	0.00	**1.00**	1535	629	777
	Tery_1667	isiA	iron-stress induced protein A, photosystem antenna protein-like, isiA	1.72	1.15	2.06	0.78	0.20	1.04	0.00	0.13	0.00	0.00	0.57	0.00	55	105	149
	Tery_1953	fur	Ferric uptake regulator	1.81	0.86	1.67	0.86	-0.22	0.74	0.00	0.31	0.03	0.00	0.27	0.00	20	44	46
	Tery_1958	fur	Ferric uptake regulator	0.42	0.26	0.09	-1.26	-1.94	-3.41	0.88	0.00	0.95	0.00	0.00	**1.00**	127	50	9
	Tery_2559	flavodoxin	Flavodoxin	0.15	2.97	0.38	-2.78	1.57	-1.38	**1.00**	0.00	0.00	**0.99**	0.00	0.99	541	69	263
	Tery_2787	dps	Ferritin and Dps	2.12	0.24	0.29	1.09	-2.06	-1.80	0.00	0.60	0.92	0.00	0.00	0.78	7	25	0
	Tery_2878	feoB	ferrous iron transport protein B	1.09	1.121	1.23	0.12	0.17	0.30	0.00	0.00	0.00	0.00	0.00	0.00	81	94	130
	Tery_2879	feoA	ferrous iron transport protein A	0.38	NA	0.19	-1.38	NA	-2.43	0.79	0.00	NA	NA	0.00	0.95	17	0	0
	Tery_3222	futC	iron(III) ABC transporter, ATP-binding protein	1.08	1.79	1.96	0.11	0.84	0.97	0.00	0.00	0.00	0.18	0.41	0.00	152	174	384
	Tery_3223	futB	iron(III) ABC transporter, permease protein	2.70	1.70	5.02	1.43	0.77	2.33	0.00	**0.99**	0.00	0.15	**1.00**	0.00	38	120	254
	Tery_3377	idiA	idiA	3.27	0.37	1.23	1.71	-1.42	0.29	0.00	**1.00**	**1.00**	0.00	0.00	0.00	413	1434	647
	Tery_3404	fur	Ferric uptake regulator	0.28	1.01	0.26	-1.82	0.02	-1.94	**1.00**	0.00	0.00	0.00	0.00	**1.00**	221	57	71
	Tery_3943	Periplasmic binding protein	Periplasmic binding protein	0.82	0.88	0.71	-0.29	-0.18	-0.50	0.00	0.00	0.01	0.00	0.00	0.04	88	75	80
	Tery_4282	dpsA	Ferritin and Dps	1.21	0.22	0.26	0.27	-2.20	-1.96	0.00	0.00	**1.00**	0.00	0.00	**1.00**	491	625	158
	Tery_4448	motA/exbB	MotA/TolQ/ExbB proton channel	0.70	1.89	1.31	-0.51	0.92	0.39	0.03	0.00	0.00	0.40	0.01	0.00	57	40	99
	Tery_4449	exbD	Biopolymer transport protein ExbD/TolR	2.02	1.37	3.39	1.02	0.45	1.76	0.00	0.52	0.00	0.09	**0.97**	0.00	12	33	59
Metacaspases genes	Tery_0382	TeMC8	Putative Chase2 sensor protein, metacaspase	3.25	1.04	3.49	1.70	0.06	1.81	0.00	**1.00**	0.00	0.00	**1.00**	0.00	90	322	409
	Tery_1841	TeMC7	Peptidase C14,C caspase catalytic subunit p20, metacaspase	2.60	1.11	2.92	1.38	0.16	1.54	0.00	**1.00**	0.00	0.00	**1.00**	0.00	442	1219	1647
	Tery_2963	TeMC12	Hypothetical protein	0.64	NA	0.41	-0.63	NA	-1.30	0.25	0.00	NA	NA	0.01	0.63	5	0	0
	Tery_2058	TeMC6	Peptidase C14,C caspase catalytic subunit p20, metacaspase	2.91	0.44	1.28	1.54	-1.19	0.35	0.00	**1.00**	0.76	0.00	0.01	0.00	61	199	102
	Tery_2077	TeMC1	Hypothetical protein, metacaspase	5.31	1.08	5.91	2.41	0.11	2.56	0.00	**1.00**	0.00	0.00	**1.00**	0.00	129	747	981
	Tery_2158	TeMC11	Hypothetical+protein	2.60	1.39	3.89	1.38	0.47	1.96	0.00	**0.98**	0.00	0.01	**1.00**	0.00	41	124	214
	Tery_2471	TeMC4	Peptidase C14,C caspase catalytic subunit p20, metacaspase	2.38	1.78	4.30	1.25	0.83	2.10	0.00	**1.00**	0.00	0.04	**1.00**	0.00	266	675	1461
	Tery_2624	TeMC10	Peptidase C14,C caspase catalytic subunit p20, metacaspase	1.46	2.07	3.19	0.55	1.05	1.67	0.00	0.01	0.00	0.58	**1.00**	0.00	58	94	245
	Tery_2689	TeMC2	Hypothetical protein, metacaspase	1.98	1.12	2.27	0.99	0.17	1.18	0.00	0.46	0.00	0.00	0.88	0.00	118	253	347
	Tery_2760	TeMC5	Peptidase C14,C caspase catalytic subunit p20, metacaspase	1.84	1.49	2.90	0.88	0.57	1.54	0.00	0.27	0.00	0.04	**0.99**	0.00	49	102	189
	Tery_3869	TeMC3	WD-40 repeat containing protein, metacaspase	2.79	2.21	6.24	1.48	1.14	2.64	0.00	**1.00**	0.00	**0.97**	**1.00**	0.00	300	889	2390
	Tery_4625	TeMC9	WD-40 repeat-containing protein, metacaspase	2.82	1.54	4.36	1.50	0.62	2.13	0.00	**1.00**	0.00	0.00	**1.00**	0.00	507	1516	2826